Technical Report SL-95-23
December 1995

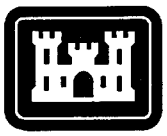

US Army Corps of Engineers
Waterways Experiment Station

A Finite Element Model for Assessment of Maglev Vehicle/Guideway Interaction

by James C. Ray, Yazmin Seda-Sanabria, Mostafiz R. Chowdhury, Stanley C. Woodson

Approved For Public Release; Distribution Unlimited

Prepared for U.S. Army Engineer Division, Huntsville

PRINTED ON RECYCLED PAPER

Technical Report SL-95-23
December 1995

A Finite Element Model for Assessment of Maglev Vehicle/Guideway Interaction

by James C. Ray, Yazmin Seda-Sanabria,
Mostafiz R. Chowdhury, Stanley C. Woodson

U.S. Army Corps of Engineers
Waterways Experiment Station
3909 Halls Ferry Road
Vicksburg, MS 39180-6199

Final report

Prepared for U.S. Army Engineer Division, Huntsville
Huntsville, AL 35807-4301

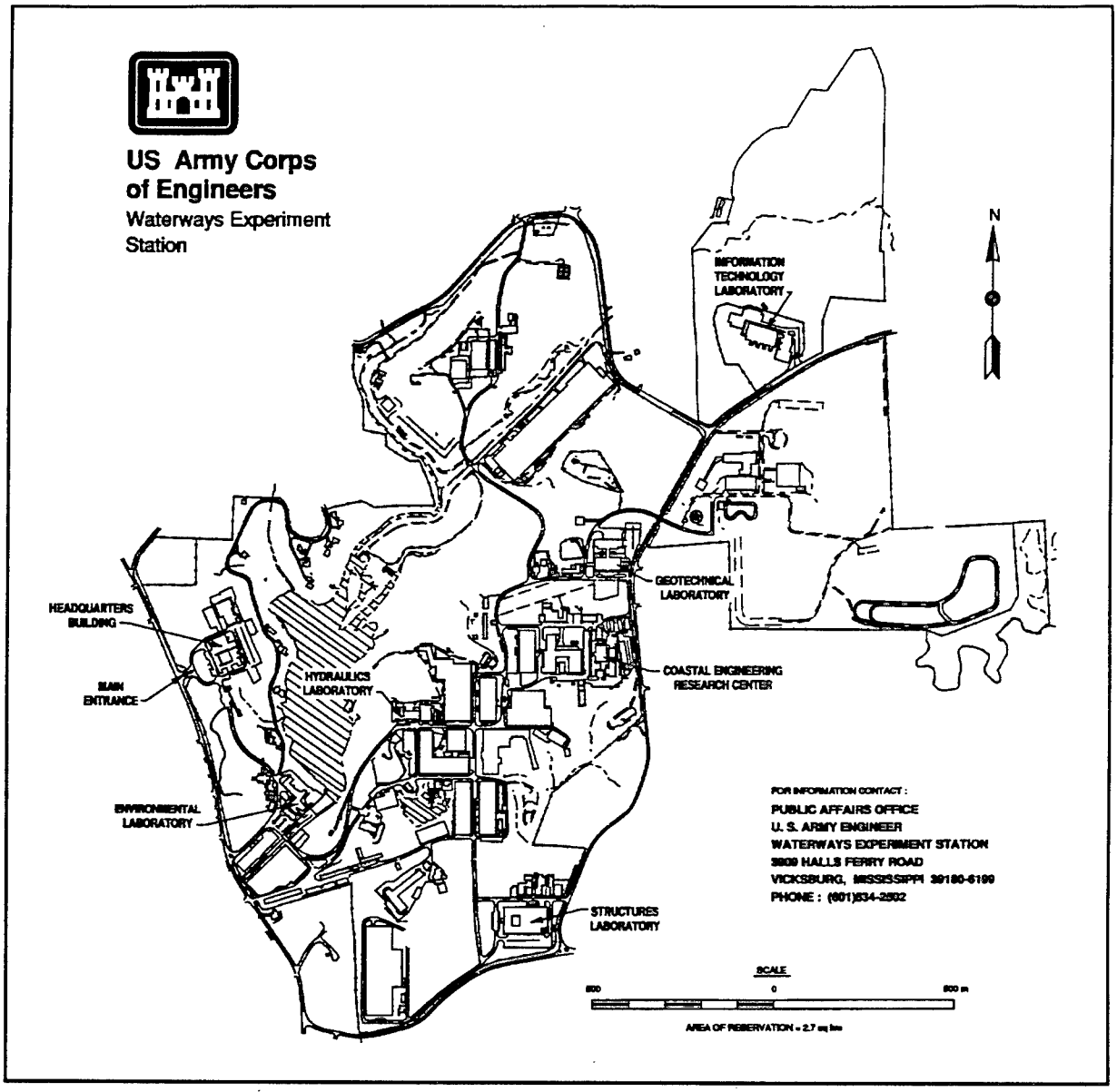

Waterways Experiment Station Cataloging-in-Publication Data

A finite element model for assessment of Maglev vehicle/guideway interaction / by James C. Ray ... [et al.] ; prepared for U.S. Army Engineer Division, Huntsville.
78 p. : ill. ; 28 cm. — (Technical report ; SL-95-23)
Includes bibliographic references.
1. Magnetic levitation vehicles. 2. High speed ground transportation — Design and construction. I. Ray, James C. II. United States. Army. Corps of Engineers. Huntsville Division. III. U.S. Army Engineer Waterways Experiment Station. IV. Structures Laboratory (U.S. Army Engineer Waterways Experiment Station) V. Series: Technical report (U.S. Army Engineer Waterways Experiment Station) ; SL-95-23.
TA7 W34 no.SL-95-23

Contents

List of Figures

Preface

The research reported herein was sponsored by the U.S. Army Engineer Division, Huntsville. Mr. Rick Suever was the Technical Monitor.

All work was carried out by Mr. James C. Ray, Ms. Yazmin Seda-Sanabria, Dr. Mostafiz R.Chowdhury, and Dr. Stanley C. Woodson, Structural Mechanics Division (SMD), Structures Laboratory (SL), U.S. Army Engineer Waterways Experiment Station (WES), under the general supervision of Mr. Bryant Mather, Director, SL; Mr. John Ehrgott, Assistant Director; and Dr. Reed Mosher, Chief, SMD. The work was conducted during the period January-December 1995 under the direct supervision of Mr. Ray.

At the time of publication of this report, Director of WES was Dr. Robert W. Whalin. Commander was COL Bruce K. Howard, EN.

1 Introduction

Background

Practical superconducting magnetic levitation (Maglev) was pursued in the United States in the 1960's. Development of the concept continued for a short time in the United States; but in the 1970's, Federal funding for Maglev vanished and development in the United States effectively ceased. Foreign governments, however, continued development of the Maglev concept. Today, both Germany and Japan have working prototypes.

As a result of the evolving foreign technology and increasing transportation needs, the United State's interest in Maglev was renewed in 1990. In December 1990, the National Maglev Initiative (NMI) was formed in conjunction with the Department of Transportation, the Corps of Engineers, and the Department of Energy. Its purpose was to evaluate the potential for Maglev to improve intercity transportation in the United States and to determine the appropriate role for the Federal Government in advancing this technology.

As part of its evaluation, the NMI sought industry's perspective on the best ways to implement Maglev technology. The NMI awarded four System Concept Definition (SCD) contracts to teams led by Bechtel Corp., Foster-Miller, Inc., Grumman Aerospace Corp., and Magneplane International, Inc. These contracts resulted in thorough descriptions and analyses of four innovative Maglev concepts.

The NMI also formed an independent Government Maglev System Assessment (GMSA) team. The GMSA team consisted of scientists and engineers from the U.S. Army Corps of Engineers (USACE), the U.S. Department of Transportation (USDOT), and Argonne National Laboratory (ANL), along with contracted transportation specialists. The team assessed the technical viability of the four SCD concepts, the German TR07 Maglev design, and the French TGV high-speed train (Lever 1993). Part of these assessments included the use of existing analytical tools to study and compare various high-risk or high-cost concerns related to each system, such as the guideway structures, magnetic suspensions and stray magnetic fields, motor and power systems, and vehicle/guideway interaction. As a result of these assessments, shortcomings were recognized in the state of the art of available analytical tools for this purpose. To address these shortcomings, the NMI funded several

projects to further develop specific analytical tools for use in future evaluations of Maglev designs. The development of a vehicle/guideway interaction (VGI) finite element model presented in this report was part of that effort. VGI refers to the dynamic interaction (coupling) between two separate dynamic systems: the Maglev vehicle and its supporting flexible guideway. The vehicle response is affected by the roughness and flexibility of its supporting guideway; and the guideway responds when acted upon by the passage of the vehicle and its time-varying suspension forces. In order to accurately predict the performance of either the vehicle or the guideway, the dynamic interaction between the two must be considered.

Previous work accomplished as a joint effort between the U.S. Army Engineer Waterways Experiment Station (USAEWES) and the Volpe National Transportation Service Center (VNTSC) resulted in a methodology for modeling the VGI effects, referred to herein as the VGI Model (Ray and Chowdhury 1994). However, this modeling concept required the use of two separate computer programs, one maintained by the VNTSC and one by the USAEWES, which made use of the VGI model by other agencies difficult. Other minor shortcomings were discussed by Ray and Chowdhury (1994). To address the shortcomings, the WES developed an "all-in-one" finite element (FE) model for VGI, referred to herein as the FE Model. The development, validation, and use of the FE Model are described herein.

The FE Model has two distinct applications: it can be used to predict the vehicle ride quality for a given vehicle and guideway design, and to accurately predict the dynamic deflections and stresses experienced throughout the guideway structure as a result of a vehicle passage. Ride quality results are necessary to design a vehicle suspension system and to determine the guideway stiffness required to meet specific ride quality criteria. Dynamic structural analyses are necessary to produce safe, economical, and accurate guideway designs.

Objective

The objective of this work was to develop a FE Model for the assessment of the dynamic interaction between moving Maglev vehicles and their supporting guideways. The intended use of the model is to predict the ride quality and stability of Maglev vehicle/guideway designs and the dynamic response of the guideway as a result of vehicle passage.

Scope

The ABAQUS finite element code (HKS, Inc. 1992) was chosen as the basic analysis tool for the VGI study since it offers a unique three-dimensional (3-D) "slideline" contact element. This element was used to provide the required frictionless-moving interaction surface between the forward-moving multi-degree-of-freedom (MDOF) Maglev vehicle and its supporting guideway. The use of the slideline elements for this purpose was validated through application to a simplified problem, consisting of a simple beam traversed by two interconnected spring masses. The problem was solved for both a two-dimensional (2-D) beam mesh and for an equivalent 3-D slab mesh. The 2-D beam results were validated by comparison to the application of a closed-form solution ; the 3-D slab results were validated by comparison to results from the VGI Model previously developed by Ray and Chowdhury (1994).

Once validated, the FE Model was applied to the Foster-Miller System Concept Design (SCD) as described in Foster-Miller (Foster-Miller 1992). As a result of previous work, a detailed 3-D shell-element mesh of the Foster-Miller guideway had already been developed and analyzed using the VGI Model (Lever 1993 and Ray and Chowdhury 1994). A 3-D FE mesh of the Foster-Miller vehicle was developed and applied to the guideway mesh through use of the slideline elements. The results from this analysis were validated by comparison to the similar analyses by Ray and Chowdhury (1994).

The dynamic problem solution using the detailed 3-D guideway mesh described above required a large amount of computer time. Therefore, a simplified beam-element mesh of the Foster-Miller guideway was also developed in order to demonstrate the accuracy and usefulness of the FE Model even when computer resources are limited. This beam-element mesh was also used to study application of the model to a multispan guideway and a curved guideway.

2 FE Model

General

VGI analysis involves the solution of two completely separate and complex dynamic systems: the vehicle with its unique 3-D suspension and control characteristics; and the guideway with its unique 3-D flexibility characteristics. Figure 1 demonstrates the general VGI problem. As the vehicle moves along the guideway, it is acted upon by external forces and by the suspension system forces which cause linear and rotational accelerations of the vehicle. If the vehicle has appreciable flexibility, the forces may also cause considerable deformation of the vehicle body. The suspensions react to the vehicle body and guideway surface characteristics and motions, and produce suspension forces acting on the vehicle and on the guideway. The guideway beams deflect dynamically in response to the moving, unsteady suspension forces and the reaction forces and moments generated at the support. Finally, the support motions are determined by the support and foundation dynamic characteristics and the guideway beam forces and moments.

This strongly coupled problem has been solved in the past in different ways, most of which required numerous simplifying assumptions to make the solution feasible. Richardson and Wormely (1974) provide a summary of many of these solution techniques. Ray and Chowdhury (1994) also provide a discussion of a decoupled VGI model that combines the FE guideway analysis with the force-time histories of the vehicle analysis. The FE Model presented herein offers a solution to many of the shortcomings of the VGI model.

The general FE method of structural analysis is well documented in the literature, thus its theory will not be discussed in detail herein. Gallagher (1975) provides an excellent overview of the FE methodology. The basic concept of the method, when applied to problems of structural analysis, is that a continuum (the total structure) can be modeled analytically by subdividing it into regions (the finite elements). The behavior of each of these regions is described by a separate set of assumed functions representing the stresses or displacements over that region. These sets of functions are often chosen in a form that ensures continuity of the described behavior throughout the complete continuum. Much like other procedures utilized in the numerical solution of structural mechanics problems, the FE method requires the formulation and solution of systems of algebraic equations. The special advantages of this method reside in its

suitability for automation of the equation formulation process and in the ability to represent highly irregular and complex structures and/or loading situations.

The FE Model described in this report is based upon the ABAQUS FE code. The Model consists of three basic parts: an FE mesh of the guideway, an FE mesh of the Maglev vehicle(s), and a definition of the interaction surfaces (known as "slidelines") which are used to model the interaction between the guideway and vehicle meshes. Each of these parts of the Model is described in detail in the following paragraphs.

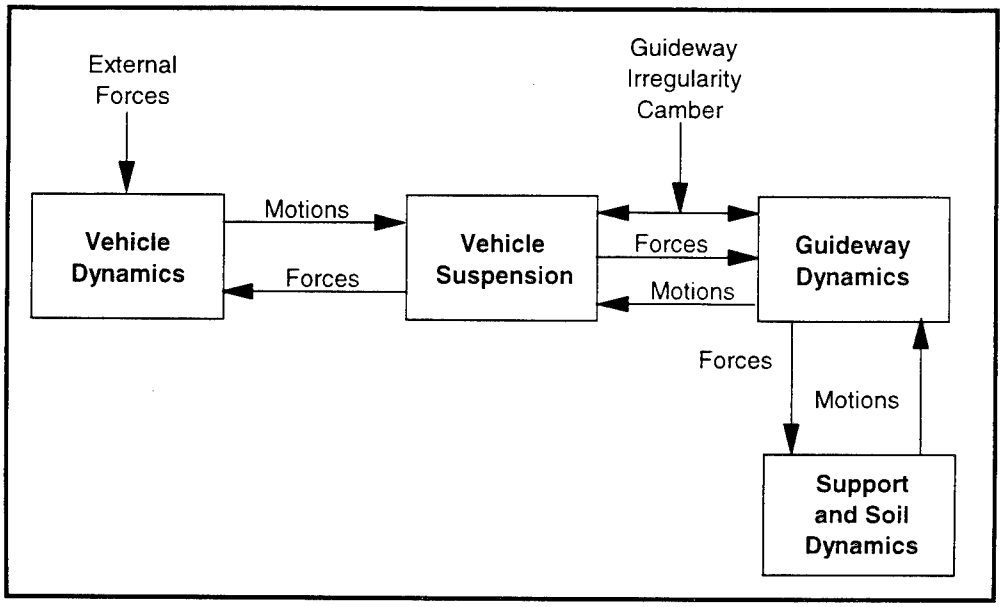

Figure 1. General VGI solution

Guideway FE Mesh

In order to perform an FE analysis of any structural system, it must first be discritized into a "mesh" of finite elements. The boundaries of the elements are defined by nodes. The elements composing the mesh of a given structure may be of any size and number. However, the refinement of the mesh (i.e., number of elements and nodes composing the mesh) must be carefully chosen in each case in order to obtain accurate results with the greatest economy of computational requirements. Numerous guidelines are provided in the literature for the effective idealization of structures with finite elements. Meyer (1987) provides an excellent discussion of this topic for conventional structures. For use in the FE Model, the size of the elements must be based on several other primary factors, as will be discussed below.

The FE mesh must be of such refinement that its solution will correctly reproduce the characteristic mode shapes of the real structure which are likely to be excited by the loads. For the case of a Maglev vehicle traversing a well-

constructed (i.e., smooth) guideway, the loading frequency is mainly a function of the vehicle crossing speed and the bogie spacing. It will depend, to a limited extent, upon the bogie load variation resulting from such factors as guideway roughness and misalignment. However, these load variations will be of very high frequency, generally small in magnitude for smooth guideways, and thus will have little affect on the overall guideway response. Richardson and Wormely (1974) indicate that for guideways with k equal spans, the number of modes important for accurate displacement calculations will be equal to k and that for bending moment and stress can be greater than $3k$. Thus, for a single-span beam guideway, the mesh should be sufficiently detailed to accurately represent the first 3 bending modes (all in the same global direction) if moments and stresses are to be determined. A minimal mesh of this type is depicted in Figure 2.

If a study of localized deflections and stresses is desired, a more detailed mesh of the guideway must be used. Note, however, that the high-frequency modes associated with localized responses will only be excited if the passing vehicle has high frequency loads associated with it. Significant loads of this nature are often not produced from soft-sprung Maglev-type suspensions. Therefore, complex localized deflections and stresses can often be most efficiently studied using a very detailed mesh in combination with static load applications. However, when the study of the dynamics of the guideway system are the main interest in the analysis, a considerably coarser mesh can be utilized instead.

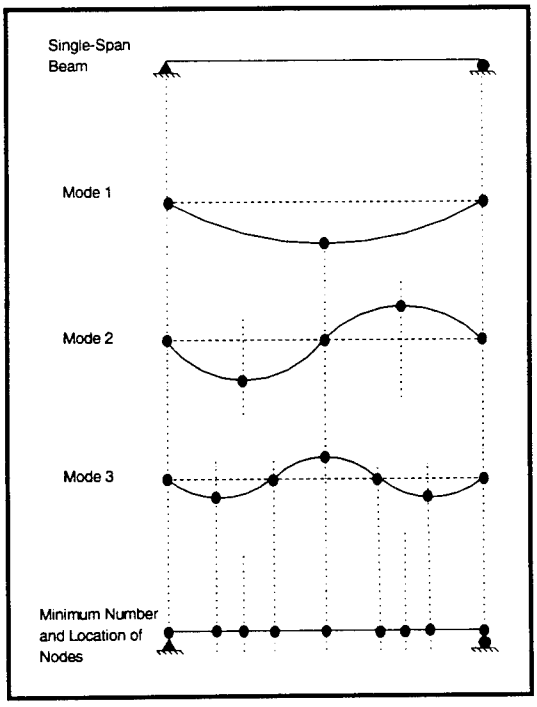

Figure 2. Minimal mesh to represent a single-span guideway

Vehicle FE Mesh

Maglev vehicles may be modeled in any desired manner and to any desired accuracy using finite elements. A simple and yet accurate method is to use solid elements combined with rotary elements, as it is shown in Figure 3. The solid elements should include the distributed mass of the vehicle and the effect of gravity on it, while the rotary elements can account for the vehicle's flexibility and bounce dynamics. The rotary elements, if located at the center of mass of the vehicle, can be used to model the vehicle's pitch inertia. The linkage between multiple vehicles can be modeled with simple spring and damper elements or with flexible 3-D solid elements.

The vehicle bogies can be modeled using beam elements. Passive suspension systems can be modeled using linear spring and damper elements. Active suspension systems can be represented by springs with predefined equations that account for variable stiffnesses. The magnetic gap may be modeled with springs and dampers (as shown), or by using the **INTERFACE* option card available in the ABAQUS code, which defines the "softened" contact between the slideline elements, as discussed below.

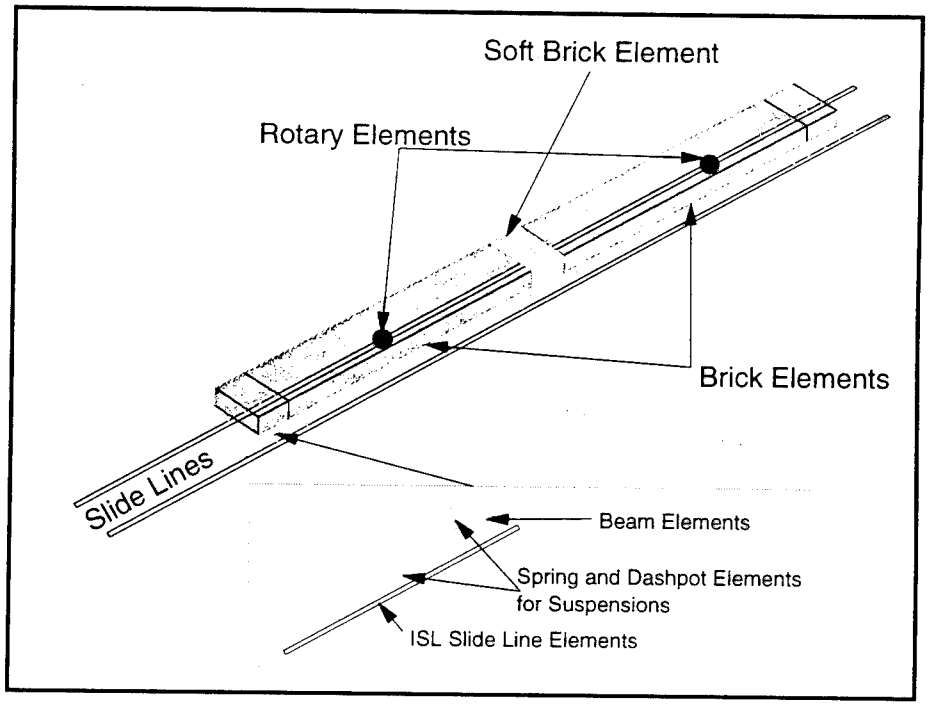

Figure 3. FE mesh of A maglev vehicle

Slideline Elements

The slideline elements available in the ABAQUS elements library are the cornerstone of the FE Model discussed in this report. These elements allow for the representation of the interaction between deformable structures along a path predefined by the slidelines, where separation and/or sliding of a finite amplitude, and even arbitrary rotation of the surfaces may possibly arise. The use of the **SLIDELINE* option card in ABAQUS is fully described by HKS Inc. (1992). It will only be briefly described in the remainder of this section.

Modeling the interaction between deformable structures requires the location of areas of contact and the solution for the surface tractions between the structures in those areas (refer to Figure 4). These tractions are considered in a local basis system defined by the normal to the contacting surfaces, n, and two orthogonal surface tangents, t_1 and t_2 (refer to Figure 5). For 2-D slidelines, t_1 is the tangent to the surface in the plane of the model. In the direction of the normal between the surfaces, the surfaces may be considered "hard" or "softened." The "softened" assumption models the presence of a local deformable layer between the surfaces, whose stiffness increases rapidly as the surfaces come into contact. The ABAQUS code assumes that the surfaces are "hard" unless softened surfaces are specified. The tangential surface tractions may be defined to include various types of frictional contact or may be neglected.

Slideline elements use a "master-slave" concept to enforce the contact constraint. The surface on which the slideline elements interact is known as the "slave" surface. A specific set of nodes is then defined as the "master" surface. The slideline elements (or the "slave" surface) slide over the nodes-defined slideline (or "master") surface. The nodes of the slideline elements are constrained so as not to penetrate into the "master" surface. Generally, the "master" surface is chosen as the surface belonging to the stiffer body if the materials interacting are of different kind. Alternatively, it can be that surface having the coarser meshing.

The 3-D slideline elements can be used to model the interaction between two deforming 3-D bodies which may come into contact along certain specific planes. They are slideline elements in the sense that they assume that the relative motion of both surfaces is predominantly along a line. This line of interaction is defined by attaching slideline interface elements to the surface of one of the bodies in a predefined plane (that is, assumed to intersect the surface orthogonally) and associating these elements with a set of defined slideline nodes in the same plane. Relative motion along the line of interaction can be arbitrarily large, but relative motions out of the plane containing the line of interaction are neglected and must be small compared to typical element sizes on the surface (Figure 6).

The nodes composing the slidelines (i.e. the "master" surface) should be defined in the ABAQUS input file in an appropriate order such that they describe a continuous line. At any point along the slideline, the direction of its tangent, t , follows the direction of the segments forming the line whose

connectivity goes from the first node entered to the second, from the second to the third, and so on until the last node forming the line is reached. The slideline outward normal, n, to the body connected to the slideline follows from $n = s \times t$, where s is the normal to the contact plane as specified in the **INTERFACE* option card of the input file (Refer to Figure 7).

Based on the above description of the **SLIDELINE* option, its usefulness for modeling VGI in a Maglev system can easily be understood. The guideway and the vehicle (including its bogies and suspension systems) can be represented to any desired degree of accuracy using the FE methodology. The interaction between these two FE meshes can then be modeled with the use of slidelines. A simple depiction of this type of model is shown in Figure 8. Note that the ISL slideline elements ("slave" surfaces) are attached to the vehicle at the bottom of its primary suspension and the slideline nodes ("master" surfaces) are laid along the guideway like tracks for a train. Since linear springs are used to model the primary suspension, the "hard" contact option (described above) should be used to define the interface between the slidelines. However, if desired, the "soft" contact option, along with a "soft" definition using the **INTERFACE* option, could be used in place of springs for the primary suspension.

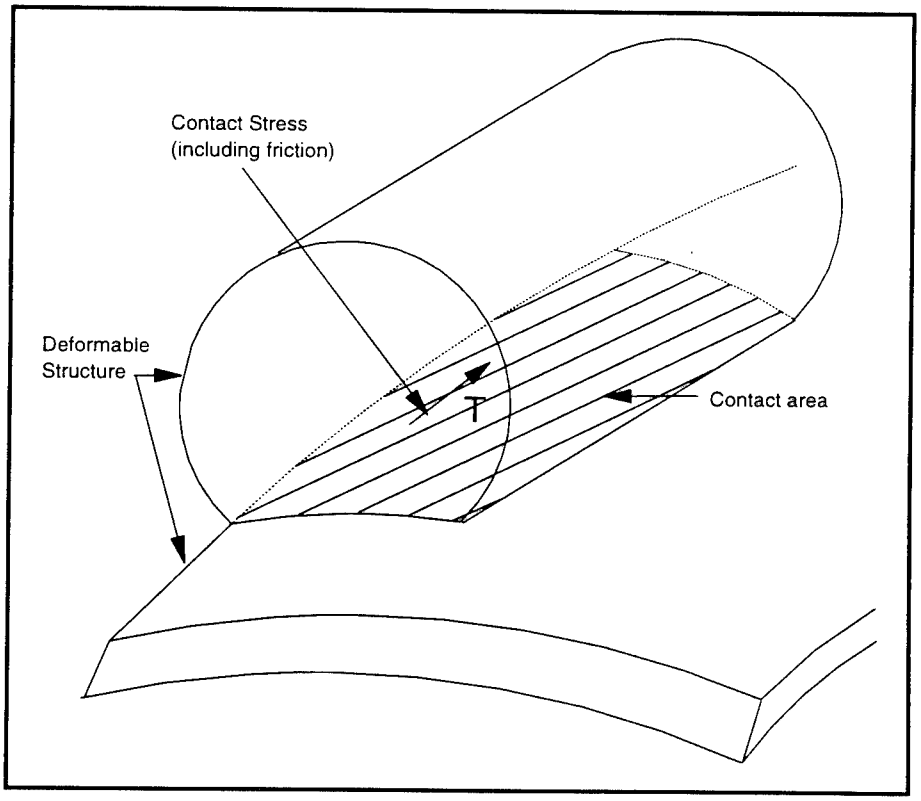

Figure 4. Contact surfaces between deformable structures

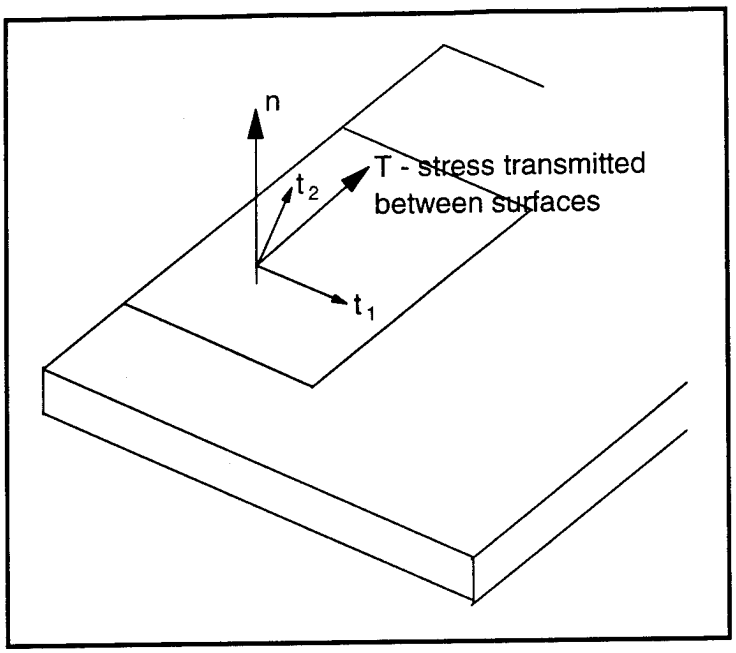

Figure 5. Local system for interface contact

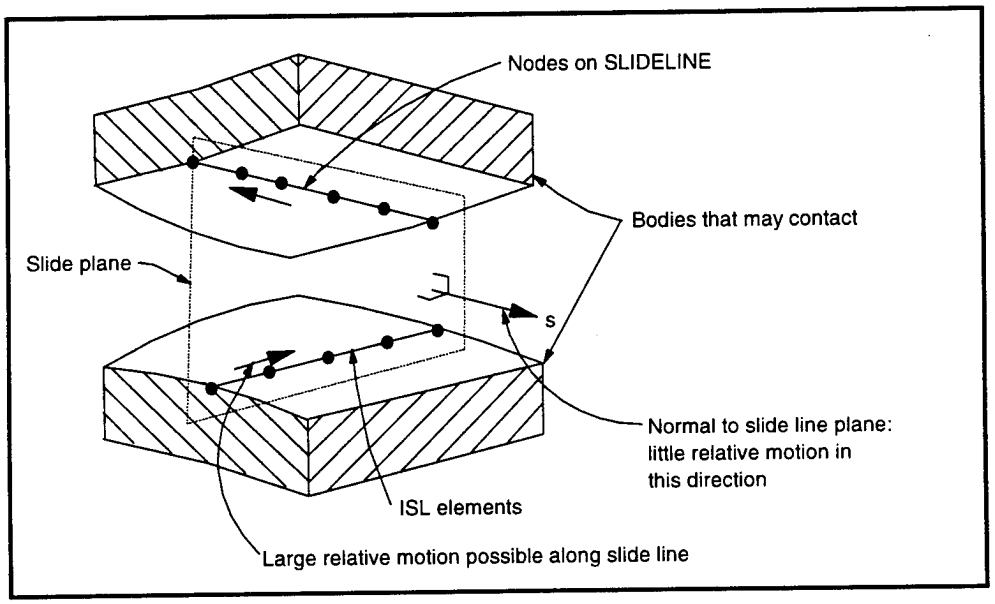

Figure 6. A slideline

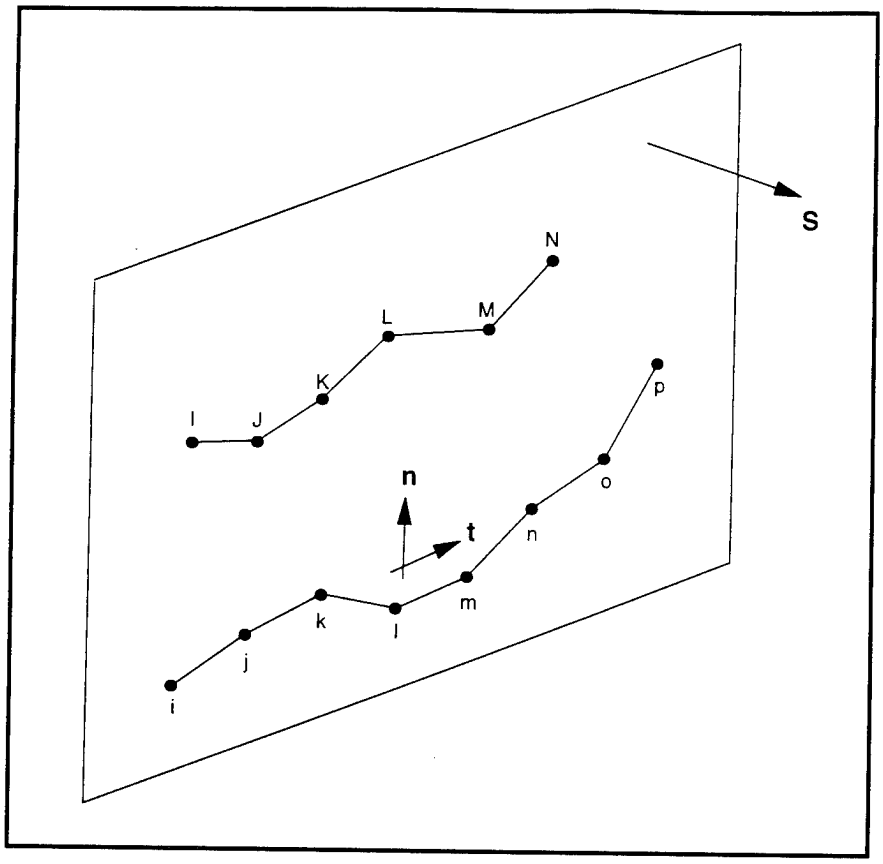

Figure 7. Three-dimensional slideline example

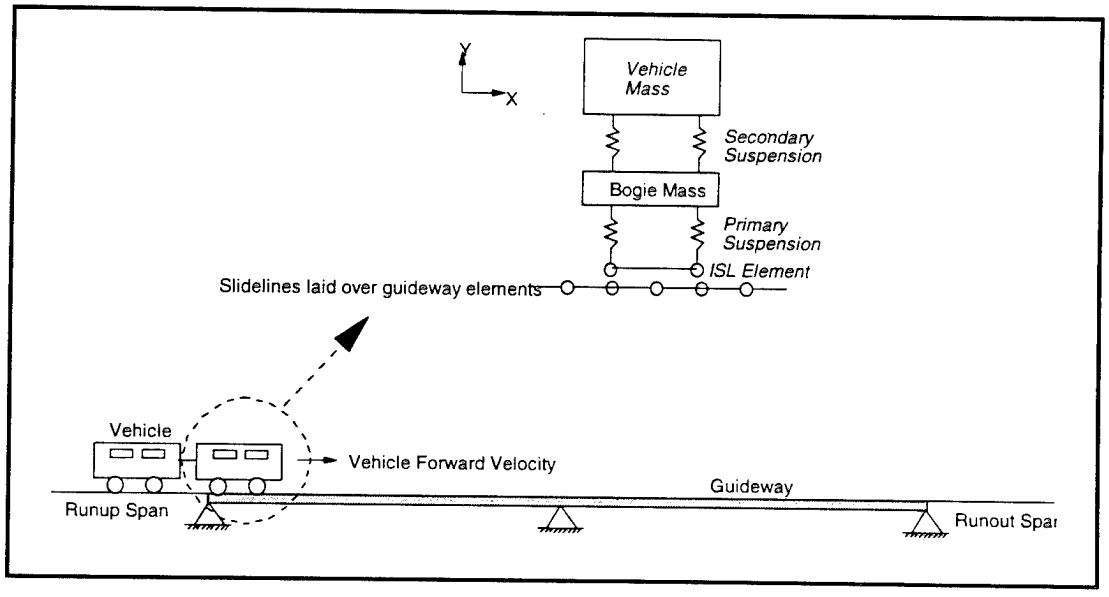

Figure 8. Application of slideline concept to a maglev system

3 Model Validation

Approach

The accuracy and validity of the FE Model were verified by comparing its results to those of a closed-form analytical solution of the simplified Maglev-type system shown in Figure 9. The system consists of a mass (representing the vehicle) suspended by both linear springs and dampers (representing the primary and secondary suspension systems), which are separated by an intermediate mass (which represents a bogie). Analytically, the vehicle was moved across a flexible simply supported beam (representing the guideway) at various speeds. The simplified representation is a two degree-of-freedom system (2-DOF system) which only considers motion in the vertical plane and represents one support point (i.e., one bogie set) of the Maglev vehicle. In reality, a Maglev system is supported at multiple locations. For an additional comparison, the response of the simplified system was also determined using the VGI model discussed by Ray and Chowdhury (1994). The application of each of these solution methods is discussed in the remainder of this chapter.

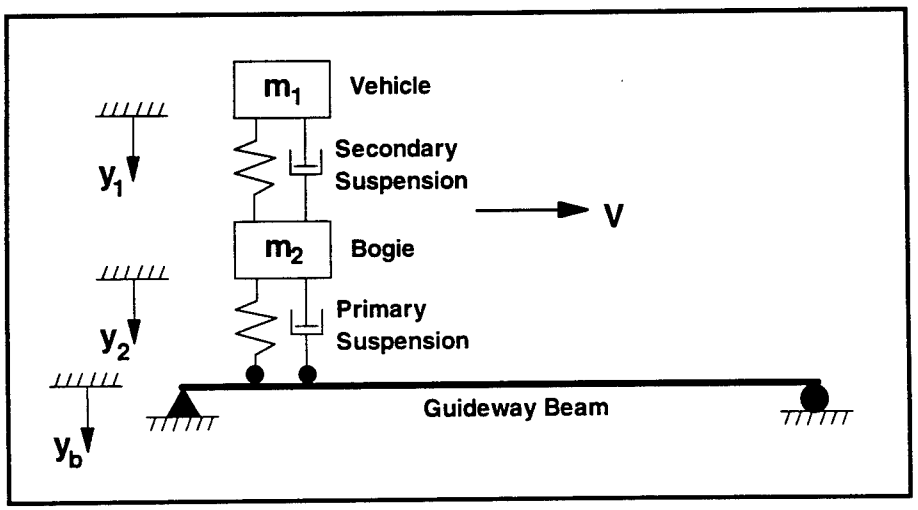

Figure 9. Simplified maglev-type system

Closed-form Solution

The 2-DOF system shown in Figure 9 can be represented by the free-body diagram presented in Figure 10. All displacements are measured from the static equilibrium position.

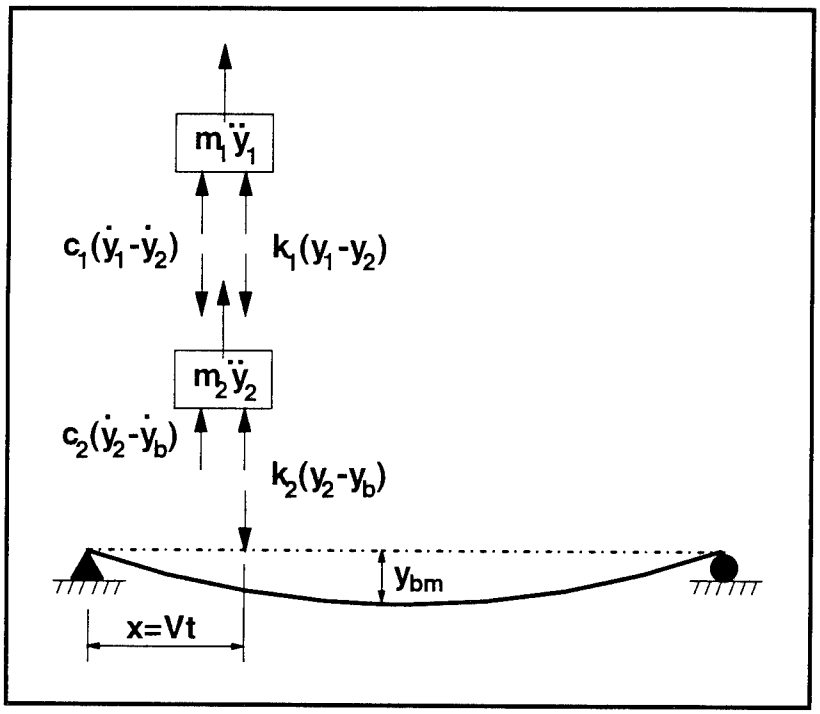

Figure 10. Free-body diagram for the simplified maglev-type system

The dynamic deflection, y_b, of a simply supported beam can be computed by using the method of Modal Superposition. The Bernoulli-Euler equation is used as the basis for this technique, and the space- and time-varying motion $y_b(x,t)$ of the beam is represented as a summation of its natural modes. This representation results in the solution given as

$$y_b(x,t) = \sum_{r=1}^{N} A_r(t)\phi_r(x) \tag{1}$$

where

A_r = modal amplitude

ϕ_r = modal shape function dependent upon the distance, x, measured from the end of the span.

The modal shapes are orthogonal over the length of the beam. For the beam shown in Figure 10, the modal shapes $\phi_r(x)$ can be approximated by,

$$\phi_r(x) = \sin\left(\frac{r\pi x}{L}\right) \tag{2}$$

Using Modal Superposition and neglecting damping, the uncoupled equation of motion for a simply supported beam subjected to a moving, constant-velocity point load, q, is expressed as,

$$\ddot{A}_r(t) + \omega_r^2 A_r(t) = \frac{q\phi_r(x)}{\int_0^L m\phi_r^2(x)dx} \tag{3}$$

where

ω_r = natural frequency corresponding to the r^{th} mode
x = instantaneous position of the point load
m = mass of the system per unit length.

For a simple beam, the integral in Equation 3 becomes $ml/2$. The applied point load, q, acting over the beam in the direction of the displacement degrees of freedom, may be expressed as:

$$q_{dynamic} = k_2(y_2 - y_b) \tag{4a}$$

$$q_{total} = k_2\left[y_2 - \sum_{r=1}^{N} A_r \sin\left(\frac{r\pi vt}{L}\right)\right] + m_1 g + m_2 g \tag{4b}$$

Substituting Equation 4 b into Equation 3, the uncoupled equations of motion of the 2-DOF system in terms of the modal displacements are obtained. The equations of motion for the system in Figure 10 are given in matrix form as follows:

$$[m]\{\ddot{y}\} + [k]\{y\} = \{f(t)\} \tag{5}$$

where

$$[m]\{\ddot{y}\} = \begin{bmatrix} m_1 & 0 & 0 \\ 0 & m_2 & 0 \\ 0 & 0 & \frac{mL}{2} \end{bmatrix} \begin{Bmatrix} \ddot{y}_1 \\ \ddot{y}_2 \\ \ddot{y}_{bm} \end{Bmatrix} \tag{5a}$$

$$[k]\{y\} = \begin{bmatrix} k_1 & -k_1 & 0 \\ -k_1 & (k_1 + k_2) & -k_2 \sin B \\ 0 & -k_2 \sin B & k_2 \sin^2 B + \frac{mL}{2}\omega_1^2 \end{bmatrix} \begin{Bmatrix} y_1 \\ y_2 \\ y_{bm} \end{Bmatrix} \tag{5b}$$

$$\{f(t)\} = \begin{Bmatrix} 0 \\ 0 \\ (m_1 + m_2)g\sin B \end{Bmatrix} \tag{5c}$$

where $$B = \frac{(\pi v t)}{L} \tag{5d}$$

For calculational simplicity, only the first modal contribution to the beam response is included. For simply supported beams, this is a reasonable simplification.

The set of equations established above were solved by using the Runga-Kutta method (Scarborough 1966). The variables were defined to represent to some extent a typical Maglev-type system, whose properties are described below:

Vehicle : $m_1 = 22{,}630\ kg$

Secondary Suspension : $k_1 = 0.60 \times 10^6\ \mathrm{N/m}$, $c_1 = 0$

Bogie Mass : $m_2 = 7{,}780\ kg$

Primary Suspension : $k_2 = 2.65 \times 10^6\ N/m$, $c_2 = 0$

Beam : $L = 25\ m$, $Width = 1.0\ m$, $Height = 2.96\ m$,

$\rho = 2{,}400\ kg/m^3$, $E = 30 \times 10^9\ N/m^2$

FE Model

The FE Model, as described in Chapter 2, was used to analyze the system previously shown in Figure 9 with the same Maglev-type system properties described above. The guideway was represented in two different ways: as a 2-D simple beam constructed from 2-node linear beam elements ; and as a 3-D slab with a vertical flexural stiffness equivalent to the 2-D beam model, and constructed from 8-node doubly curved shell elements. The equivalent mass and moment of inertia of the slab were obtained by equating the modal frequencies of both systems. This equivalency insured similar dynamic behavior for both systems.

The vehicle and bogie were represented as lumped masses coupled together with linear springs. Two sets of vehicle and bogie elements (each with half the mass of those in the 2-D model, and connected to each other by link elements) were used in the 3-D model. One set was located at each edge of the slab in order to load it more uniformly. The elements were moved over the guideway models at constant velocities. Their interaction with the guideway was modeled with 2- and 3-D slideline elements with a zero-friction contact. Both FE meshes are depicted in Figure 11. The ABAQUS input file for this analysis is provided in Appendix A.

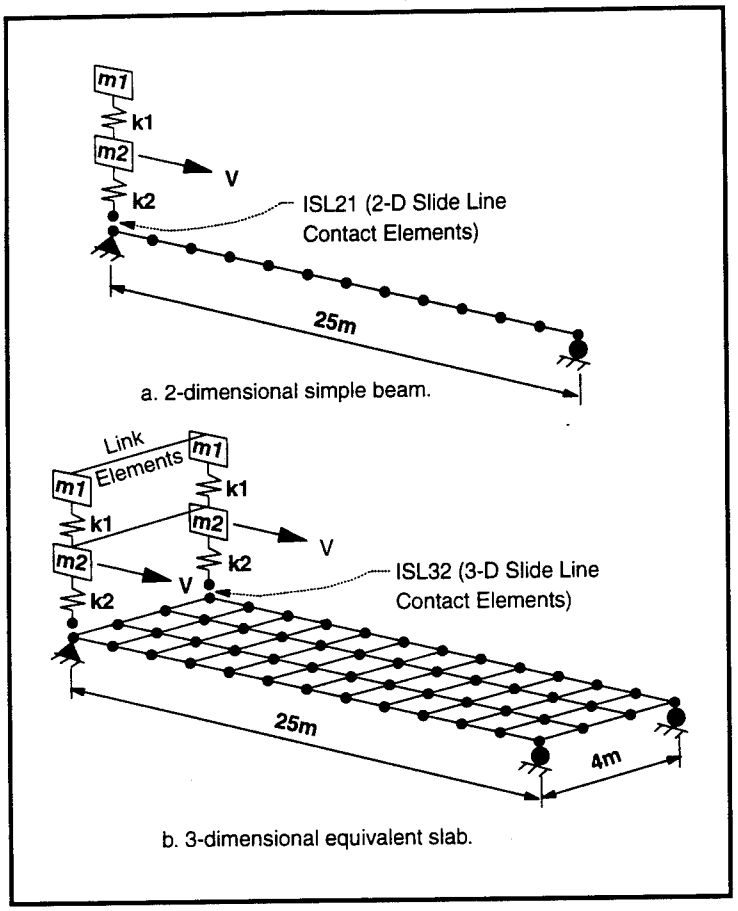

Figure 11. Meshes for FE model application

VGI Model

The response of the slab shown in Figure 11 was also obtained from the application of the VGI model, as described by Ray and Chowdhury (1994). Figure 12 shows a flowchart of the methodology that defines the application of the VGI model.

The DLOAD routine available in the VGI model serves to convert time-varying bogie forces into time- and spatially varying pressures on specific elements of the FE mesh of the structure. For the slab shown in Figure 11, the two outermost rows of elements (along the length side) were defined as the loaded elements. The bogie loads were spread out over a length (defined as "bogie length" in DLOAD) of 1m and a width of 1m, the width being determined by the widths of the loaded elements. These loads were applied as point loads in the other two analytical methods described above, but were applied as pressure loadings over a 1-m by 1-m area on each side of the slab in the VGI model.

The time-varying vehicular bogie forces at the guideway level, as required for input to the DLOAD routine, were obtained from the previously discussed closed-form solution applied to this problem. These forces are shown and discussed by Ray and Chowdhury (1994). For a normal VGI analysis using the VGI model, the bogie forces would be obtained from the VNTSC Ride Quality Analysis Code (RQAC). This code provides the vehicular accelerations (used for the ride quality assessment) and a summary of the time variation in bogie forces at the guideway level as a result of the passage of the vehicle over the flexible and randomly rough guideway.

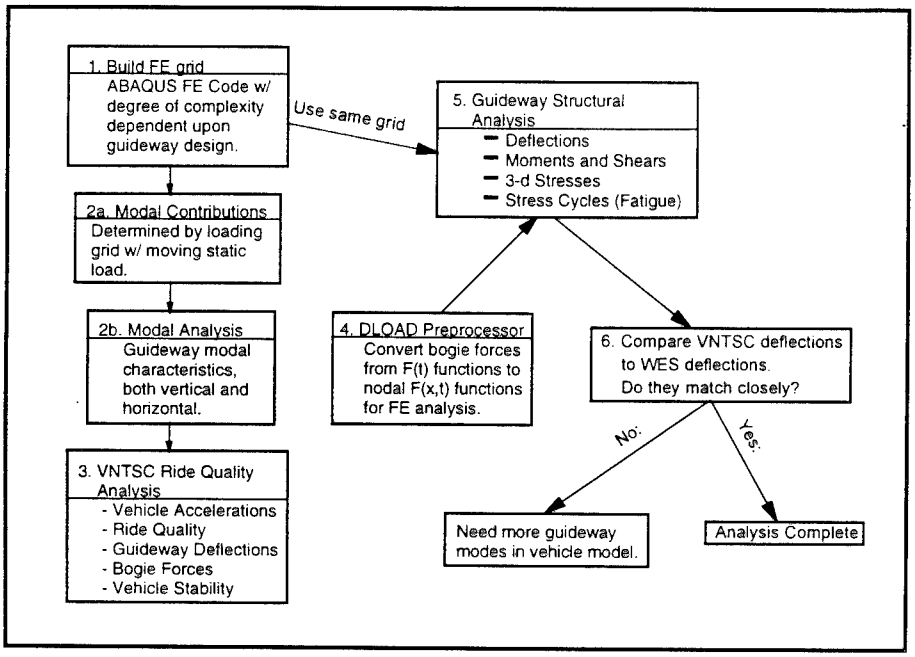

Figure 12. Flowchart describing function of VGI model

Results

Midspan beam deflections predicted by the four comparable analyses (one closed-form, two with the FE Model, and one with the VGI model) are compared in Figure 13. A vehicle velocity of v = 83 mps was used in each of the analyses. As expected, the results from both the beam and the slab FE Model analyses were almost identical, as can be seen in Figure 13. The slight variation in the curves may be attributed to the contribution of additional 3-D modes in the slab model. Likewise, the closed-form solution showed a slightly lower maximum response because only one beam flexural mode was considered in that analysis.

The slab response predicted by the VGI model lagged approximately 0.008 seconds behind that from the other analyses. This discrepancy was due to

the manner in which the integration points within the finite elements are loaded by the DLOAD routine, and the fact that no rise or decay time is used for the loadings (Ray and Chowdhury 1994). These analyses serve to verify the accuracy of the FE Model described in this report.

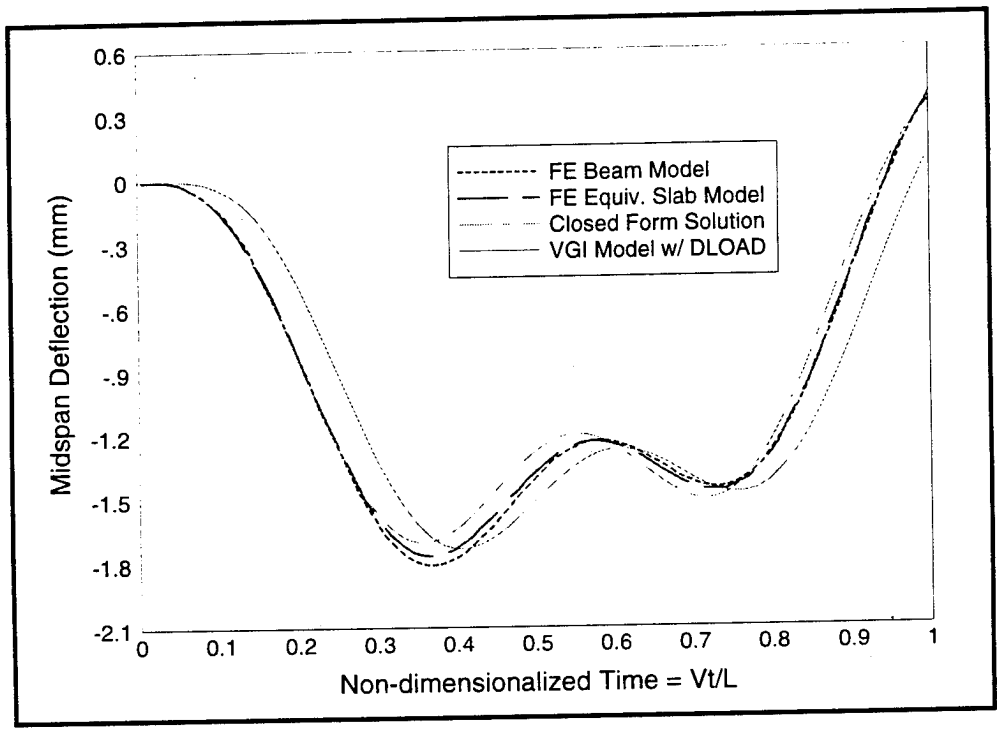

Figure 13. Comparison of analytical methods

4 Model Application

Introduction

The FE Model was applied in the analyses of the Foster-Miller SCD (Foster-Miller 1992) in order to demonstrate its utilization and to verify its applicability to actual Maglev-type systems. The Foster-Miller SCD was chosen for this demonstration because it offered both a challenging and yet somewhat generic application of the FE Model. In addition, the results can be compared to previous analyses of this system using the various applications of the VGI model discussed in Ray and Chowdhury (1994). This analysis was performed only for demonstration purposes, and the results should not be used for an actual assessment of the Foster-Miller SCD.

An FE analysis may be as detailed as desired, i.e., with either fine or coarse FE meshes. However, the degree of refinement directly affects computer time and storage requirements. For a VGI analysis of a Maglev system, the required degree of mesh refinement will depend upon the desired type of results. If one is more interested in localized stresses/deflections in the guideway, a detailed mesh of the guideway will be required. However, if one is mostly interested in the ride quality of the vehicle, the guideway mesh may be made quite coarse and more emphasis can be placed on the vehicle mesh. A coarser guideway mesh will also better facilitate longer guideways or multispan analyses. The FE Model analyses, using both types of guideway meshes (i.e., detailed and coarse), are presented in the remainder of this chapter, following a brief description of the Foster-Miller SCD.

Foster-Miller SCD

The Foster-Miller concept is an Electro-Dynamic System (EDS) generally similar to the prototype Japanese MLU002. Superconducting vehicle magnets generate lift by interacting with null-flux levitation coils located in the sidewalls of a U-shaped guideway. Similar interaction with series-coupled propulsion coils provides null-flux guidance. Its unique propulsion scheme is called a locally commutated linear synchronous motor (LCLSM). Figure 14 shows an overall view of the concept.

The baseline Foster-Miller vehicle consists of two 75-passenger modules with attached nose and tail sections. Fabrication of smaller or larger vehicles is possible by incorporating fewer or additional passenger modules. The two-car baseline vehicle was used for the demonstration presented in this report since prior analyses by Foster-Miller (Foster-Miller 1992) showed this combination to produce the worst-case loading on the guideway. The modules contain magnet bogies at each end that are shared with adjacent cars. Each bogie contains four superconducting magnets and is attached to the vehicle by a secondary suspension. The bogie spacing is approximately 24 m center-to center (Foster-Miller 1992).

The Foster-Miller guideway concept is shown in Figure 15. The guideway superstructure is a unique open-cell, integral sidewall structure constructed from modular units. Two symmetric halves are coupled together by a series of intermittently spaced truss-type diaphragms. The units are held together by posttensioning tendons that run transversely through the sections. The outer beam portions are reinforced longitudinally by a combination of pre- and posttensioned steel tendons in the lower half and fiber reinforced plastic (FRP) tendons in the upper half. The girders are erected on their pier supports as simply supported spans, and then made as two-span continuous beams with the application of external FRP posttensioning at every other support.

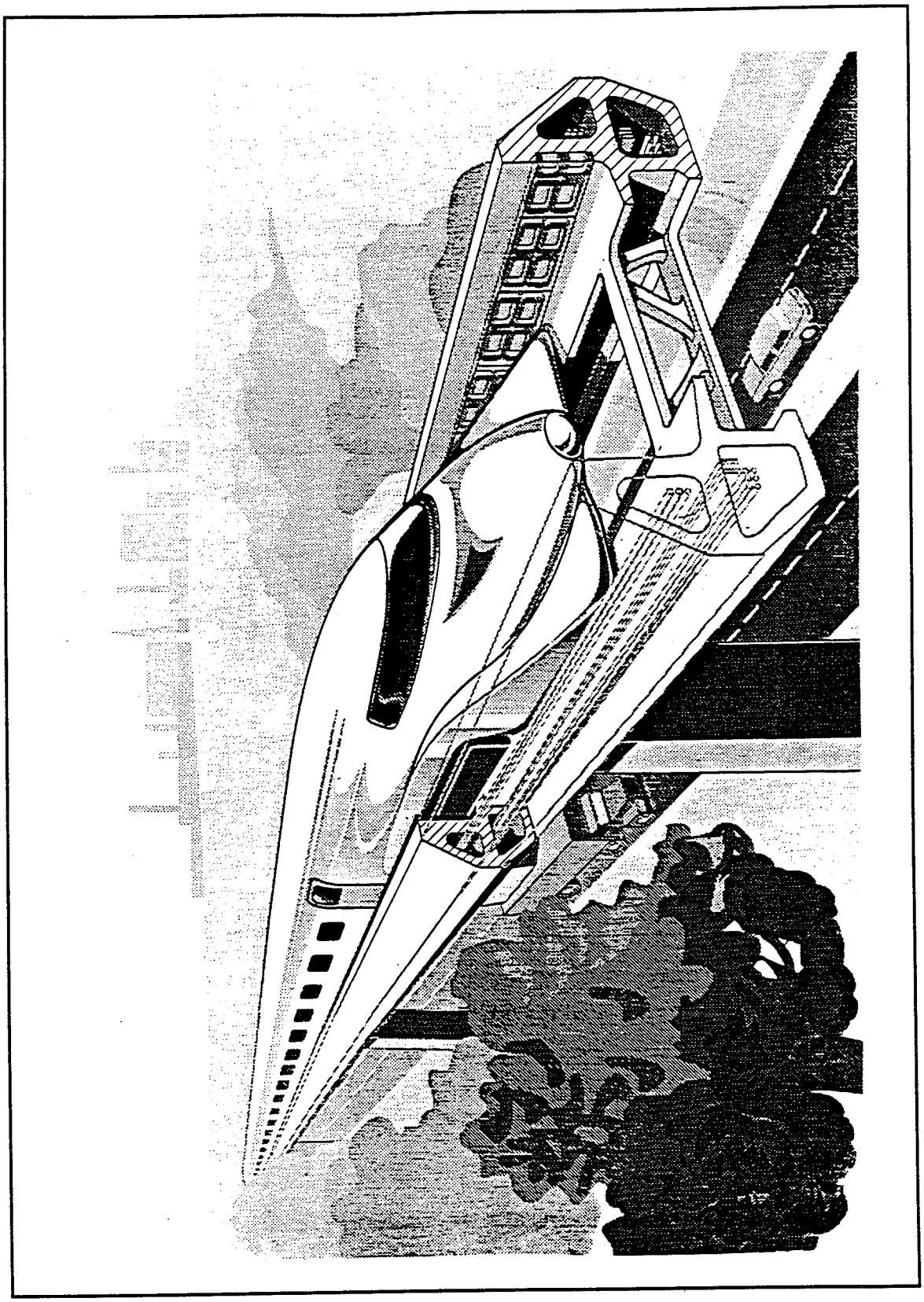

Figure 14. Foster-Miller concept

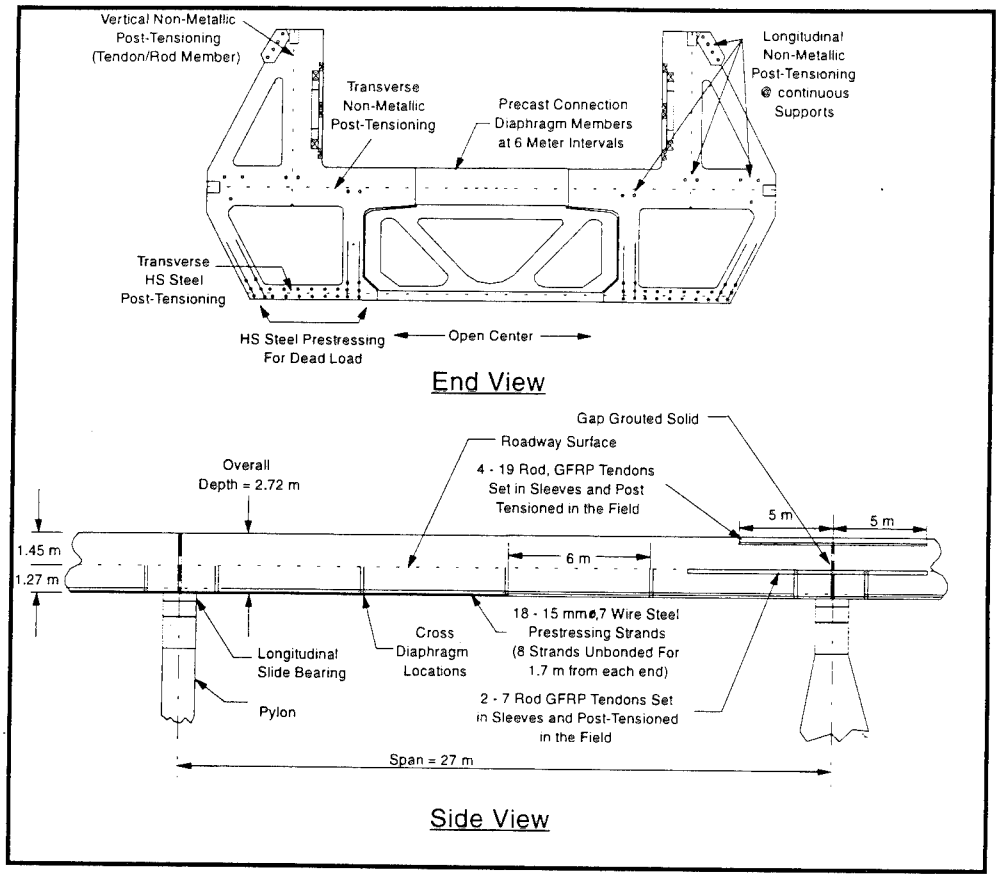

Figure 15. Foster-Miller guideway concept

Limiting Criteria for Guideway Meshes

Several limiting criteria were presented in Chapter 2 for the definition of the mesh refinement. According to the criteria, if one is interested in accurately predicting guideway deflections, then only the first two guideway modes are necessary. However, since the structural analysis plays an important role in the analysis of a maglev system (i.e., bending moments and stresses), the mesh must be dense enough along the length of the guideway to accurately represent the lower bending modes. In a Maglev-type guideway system, bending modes may be excited by the vehicular loading frequencies, which are mainly functions of vehicle speed and bogie spacing. Since the Foster-Miller guideway is a two-span continuous beam, the finite element mesh must represent the first six (i.e., $3k$, three times the number of spans) vertical bending modes of the guideway. In this analysis, only vertical loadings were to be applied to the guideway, therefore only the vertical bending modes were required. The first six general bending modes for a two-span continuous beam are shown in Figure 16. Approximately 15 to 20 elements per span are necessary to adequately represent the six modes. For example, using 20 elements per span, the maximum element length is $27m/20 = 1.4m$.

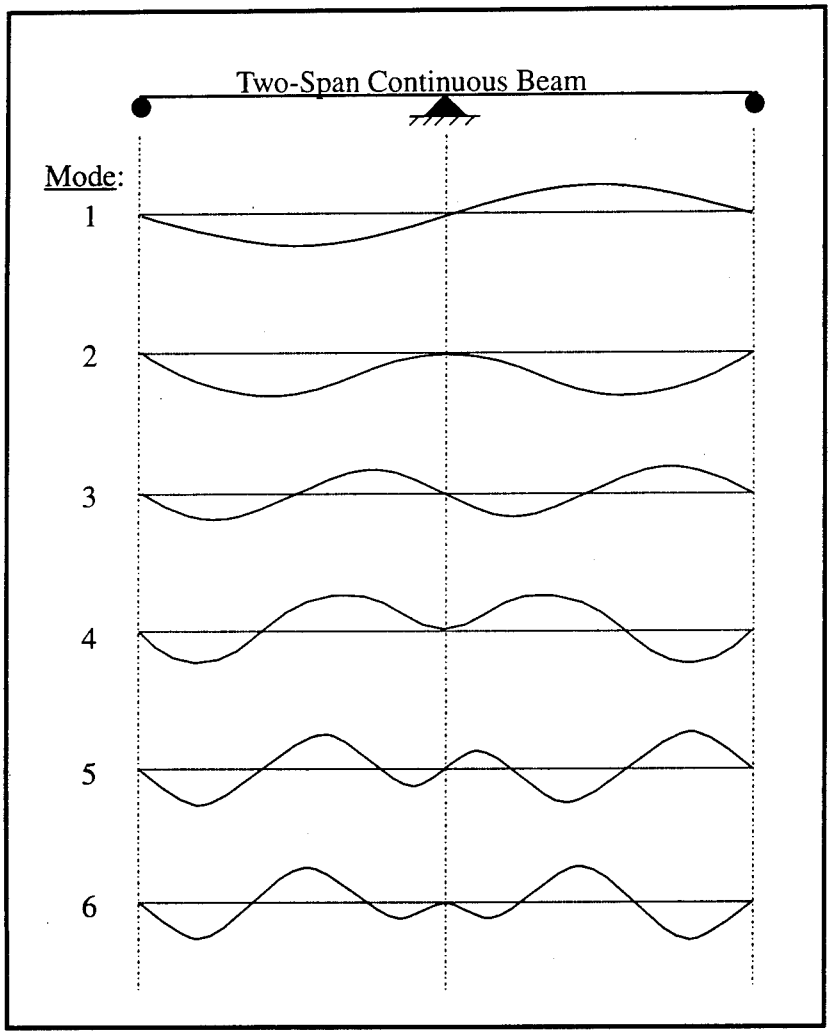

Figure 16. First six bending modes for a two-span continuous beam

Although the previous generic criteria should be sufficient to ensure accuracy of the FE mesh, it is also prudent to specifically compare the guideway loading frequency to the modal frequencies. The bogies on the Foster-Miller vehicle are spaced approximately 24 m on center. For a vehicle velocity of 140 mps (the maximum requirement for the SCD's), the guideway loading frequency will be approximately 140 mps divided by 24 m, which equals to 5.8 Hz. This frequency is very close to the first and second bending mode frequencies for the guideway (calculated based on the guideway bending stiffness and span length) and thus will primarily excite those two modes. Therefore, the above general requirement of a mesh to represent the first six bending modes is sufficient.

Analysis Using a Detailed Guideway Mesh

FE mesh

The detailed FE mesh of the Foster-Miller guideway is depicted in Figure 17. The actual guideway mesh is shown in Figure 18. The mesh contains approximately 3,000 elements and 20,000 nodes. Only the superstructure of the guideway was modeled since the substructure response would generally be of such low frequency that the vehicular ride quality would not be affected. The girder sections were modeled with eight-node thin shell elements, and the intermediate diaphragms were modeled with two-node beam elements. The length of each shell element (in the longitudinal direction of the guideway) corresponds to 0.5 m, which is within the maximum element length criteria discussed in Chapter 2.

The concrete was modeled as a linearly-elastic isotropic material since deflections and stresses in the guideway were expected to be very low, well within the elastic range. All of the prestressing (both longitudinal and transverse) in the girder sections and the diaphragms were modeled with rebar elements under initial stress conditions to represent the prestressing effect. The negative posttensioning between adjacent spans (used to make the spans continuous) was modeled as externally applied forces at 5 m from each support as shown previously in Figure 15. The longitudinal posttensioning at the mid-height of the girders (i.e. the neutral axes) was not included in this mesh. As will be discussed later in this chapter, this caused some discrepancy in results between the analyses discussed herein and those discussed by Ray and Chowdhury (1994).

The details of the vehicle as modeled are shown in Figures 19 and 20. The resulting FE mesh is depicted in Figures 21 and 22. The portion of the ABAQUS input file corresponding to the vehicle mesh generation is included in Appendix A. As shown in Figure 21, the car bodies were represented with 3-D solid elements, having distributed mass and gravity to account for the weight of the vehicle. A rotary element was used at the center of each car body to account for the vehicle's pitch inertia. Although roll inertia was not represented in this problem, its effect could have been included by using a rotary-inertia type element.

The linkage between the vehicles can be thought of as a flexible joint; it was represented with a very soft solid element. The secondary suspension system of the vehicle, which connects the car body to the bogies system, was modeled by spring and dashpot elements. The bogies were represented with linear beam elements. The primary suspension was also modeled with spring and dashpot elements.

As discussed in Chapter 2, the **SLIDELINE* option was used to provide the sliding interaction between the vehicle and the guideway system by generating "slideline" elements. These elements represented the distributed vertical interaction of the vehicle with the guideway, while also allowing for its relative motion along the guideway. As shown in Figures 21 and 22, the slideline elements were attached to the vehicle at the bottom of its primary suspension system and then moved along the guideway using the slideline nodes

located along the top surface of the guideway. The slideline nodes were also extended out in front of and beyond the end of the guideway mesh in order to provide "runup" and "runout" spans. The runup span allows the vehicle to start its forward motion while completely off of the guideway mesh, while the runout span allows the vehicle to move completely off of the guideway mesh prior to completion of the analysis. The lateral interaction between the vehicle and the guideway was also represented with slideline elements, but in this case, the slideline elements were connected directly to the beam elements that represented the bogies.

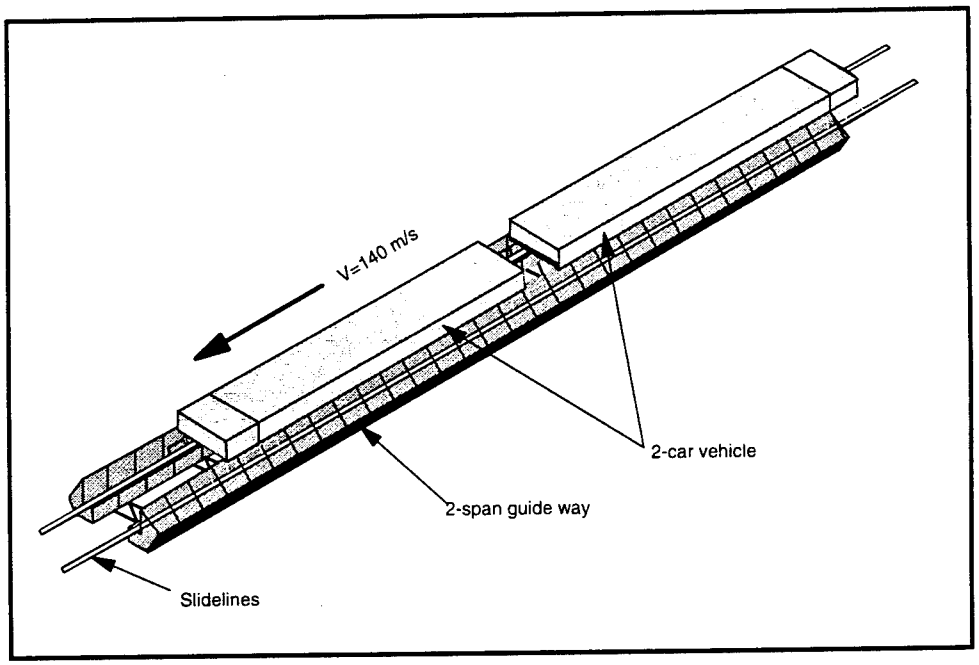

Figure 17. Depiction of detailed FE mesh for Foster-Miller SCD

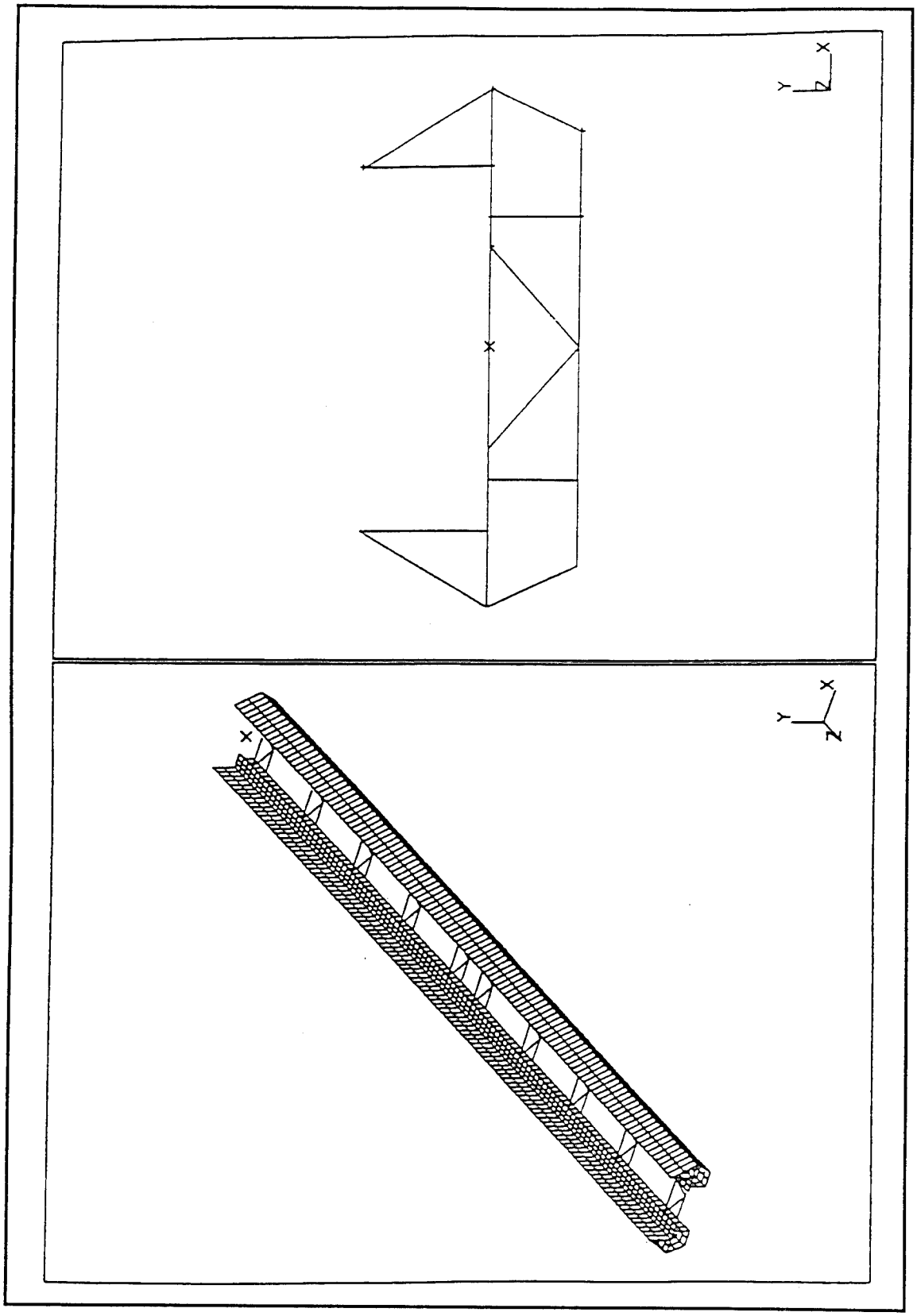

Figure 18. Detailed FE mesh of the Foster-Miller guideway

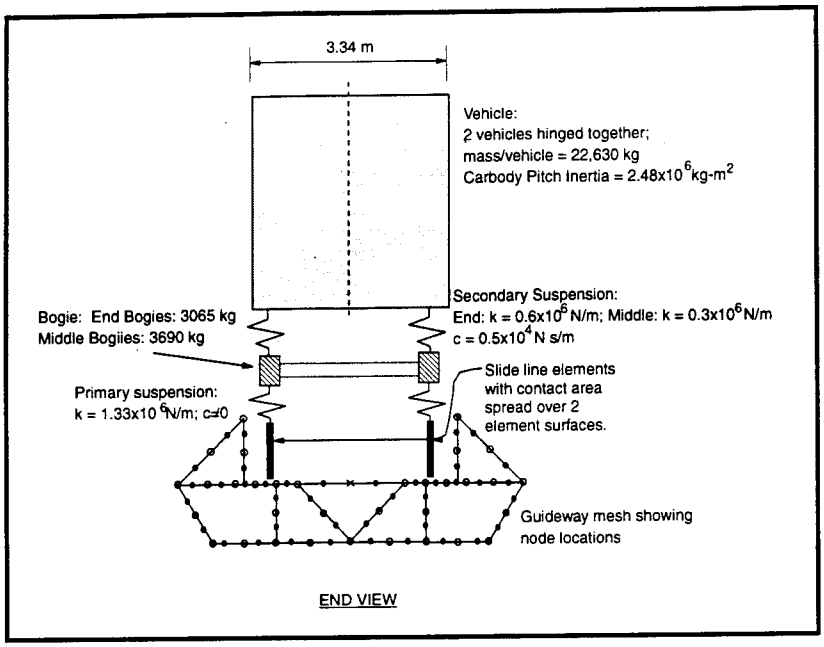

Figure 19. Details of Foster-Miller SCD as modeled (end view)

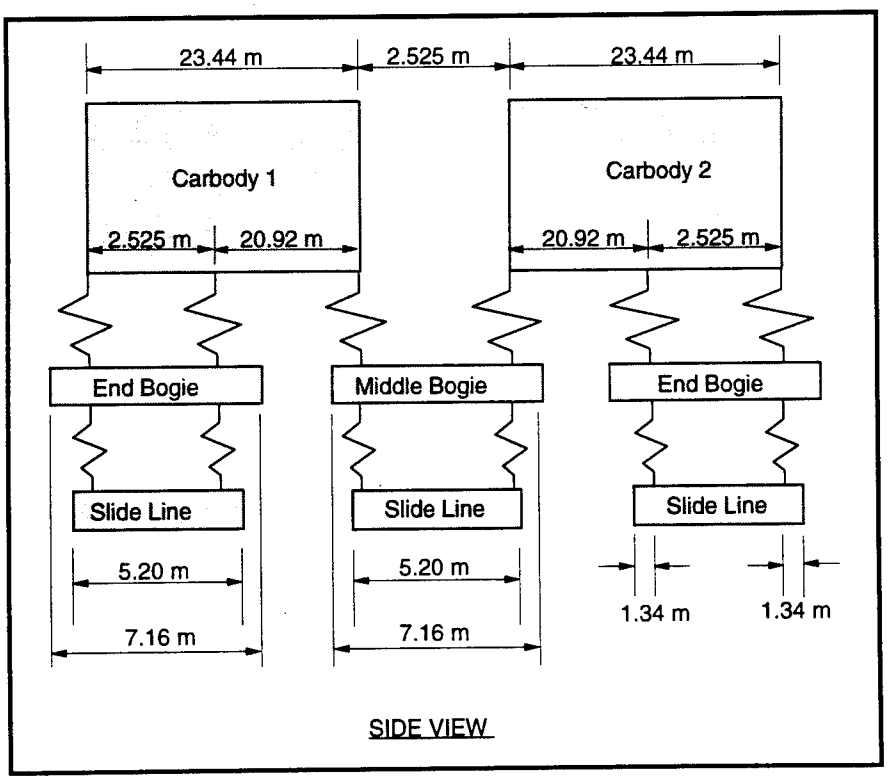

Figure 20. Details of Foster-Miller SCD as modeled (side view)

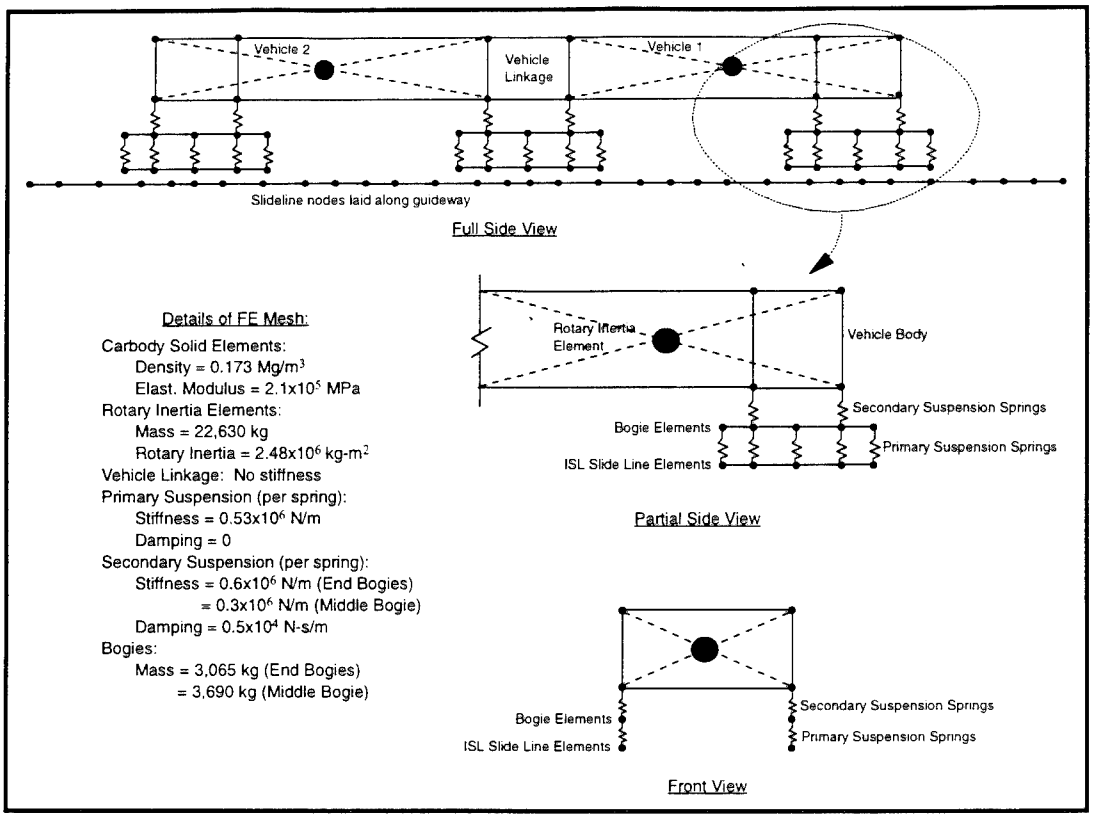

Figure 21 Depiction of FE mesh for Foster-Miller SCD

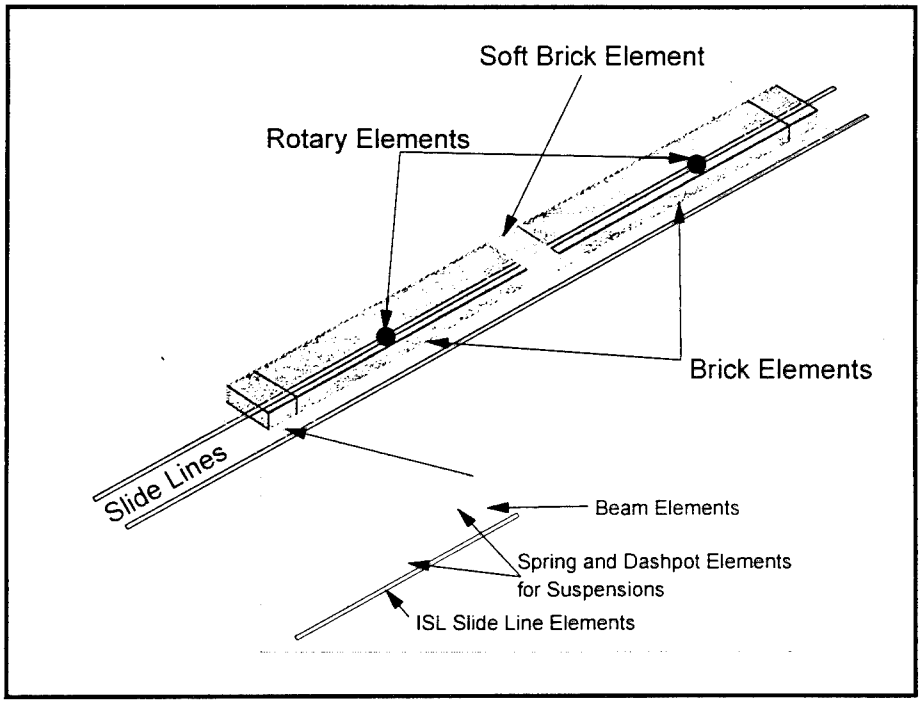

Figure 22. 3-D depiction of the Foster-Miller FE mesh

Results

The dynamic analysis of the FE mesh described above was performed using the **DYNAMIC* option available in the ABAQUS code. By applying a velocity boundary condition to all of the nodes associated with the vehicle mesh, the vehicle was effectively moved across the guideway mesh at a constant forward velocity of 140 mps. This velocity corresponds to the design speed of 500 kph for the Foster-Miller SCD. For a vehicle velocity of 140 mps, the total analysis time of 0.8 sec allowed the vehicle to move completely onto and then off of the 54-m long guideway mesh (two spans at 27 m each).

The dynamic response of the guideway is represented in Figure 23. The curves show the deflection of the midpoints of each of the adjacent 27-m-long spans. Span 1 is the span first traversed by the vehicle. The x-axis of Figure 24 was nondimensionalized by multiplying time by the vehicle velocity (140 mps) and dividing by the length of one guideway span (27 m). This process effectively shows the position of the front of the vehicle (i.e. head position) in relation to its location on each of spans 1 and 2 of the guideway. Since the vehicle mesh is also approximately 54 m long, values on the x-axis greater than 2.0 indicate that the front of the vehicle is off of the guideway mesh, but that the rear portions of the vehicle are still on it.

The continuity of the spans is evidenced in these plots by the fact that span 2 initially deflected upward due to the loading of span 1. Note that the prestressing in the guideway caused an initial upward camber (prior to the vehicle loading) of approximately 4.2 mm. In fact, even under the dynamic vehicle loading, the guideway maintained a positive upward camber. The initial camber resulted from the fact that the dead load effect on the guideway, which would have greatly reduced the camber, was erroneously omitted during the analysis. Since this work was for demonstration purposes only, the analysis was not rerun. The actual Foster-Miller design calls for zero camber under dead load.

The dynamic responses of the vehicles are compared to that of the guideway midspans in Figure 24. Vehicle 1 is the front vehicle. All deflection values were normalized to an initial zero in order to facilitate better comparison between deflection magnitudes. Only the response of the node at the vehicle's center of gravity is shown, which gives a good indication of the bounce response. While not shown, comparison of nodes at the front and back of the vehicles would represent the pitch response. As seen in Figure 25, the vehicle response is very slow due to its soft suspension, giving an indication of a smooth ride in the vehicle. Vertical vehicle accelerations would give a better indication of actual ride quality, and these may also be easily obtained from the FE analysis output if desired. It can also be seen in Figure 25 that the vehicles did not return to their initial starting positions (i.e. zero displacement) by the end of the two-span-length analysis. As a result, the vehicles would have different (i.e. nonzero displacement) initial conditions for subsequent span analyses. Therefore, this type of analysis should actually be performed over multiple guideway spans in order to fully evaluate ride quality. This is demonstrated in the next section with the simplified guideway mesh.

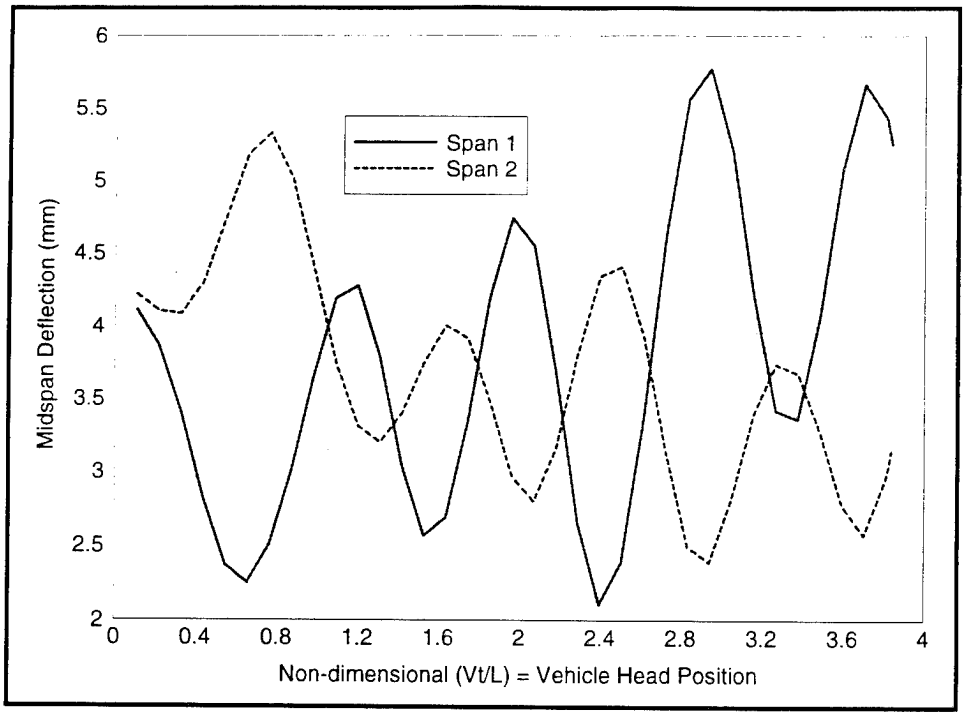

Figure 23. Guideway response to vehicle traversal

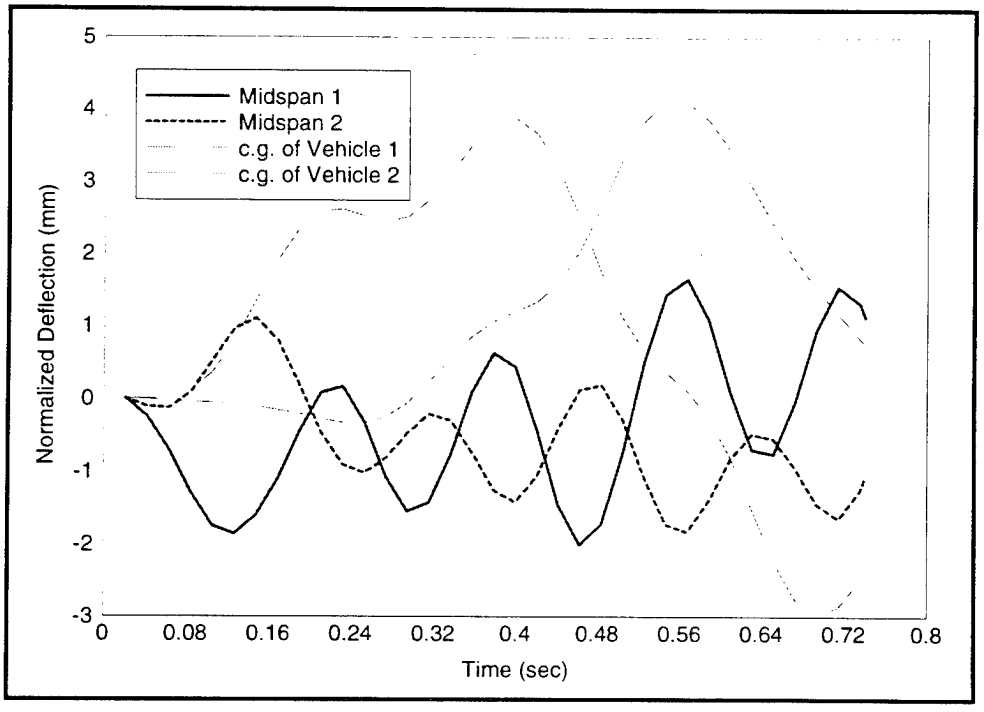

Figure 24. Comparison of vehicle and guideway response

The dynamic responses of the vehicles are compared to those of the front and rear bogies in Figure 25. The effectiveness of the secondary suspension in cushioning the vehicle response can clearly be seen. Since the primary suspensions (representative of the magnetic gaps) are between the bogies and the guideway, this type of response plot is very useful for studying potential magnetic gap/force problems. Plots of the force variation in the primary suspension springs may also be easily obtained for this purpose.

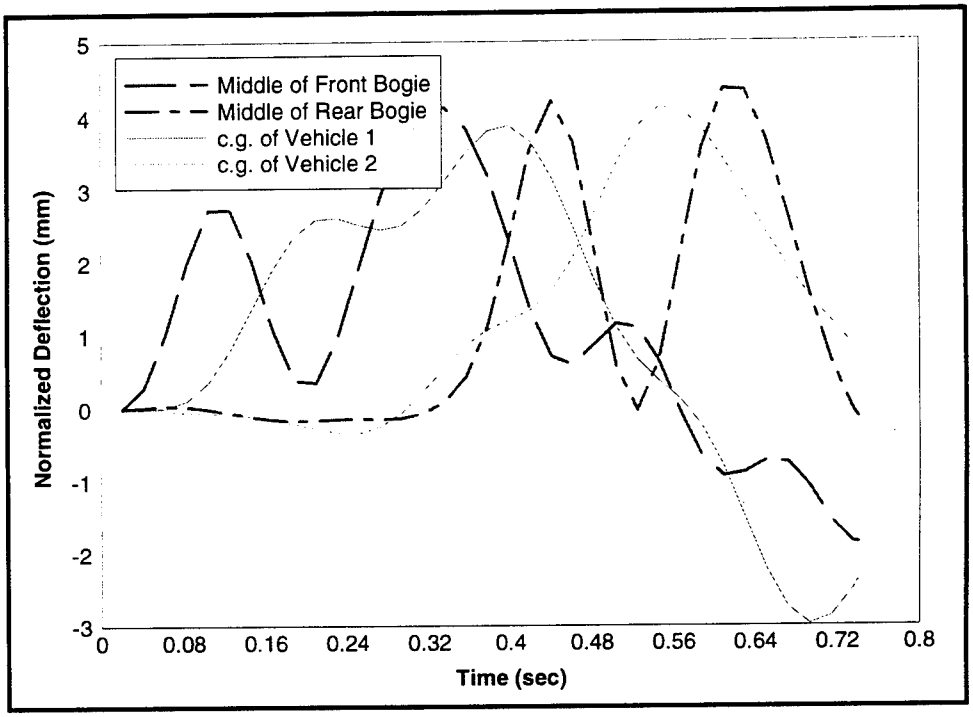

Figure 25. Comparison of vehicle and bogie responses

The results from the current analysis can be compared to the results obtained previously from the VGI model application presented in Ray and Chowdhury (1994). The two analytical methodologies compared very closely, as demonstrated in Figure 26 with a comparison of midspan guideway deflections. The deflections in Figure 27 were normalized to an initial zero position since the FE Model results showed a much larger initial precamber than that from the VGI model. This difference was due to the fact that dead load effects on the guideway were not included in the FE Model but were included in the analysis with the VGI model. This difference is also attributed to the slight differences in overall response between the two analyses. Yet in spite of this difference, the results compared very closely.

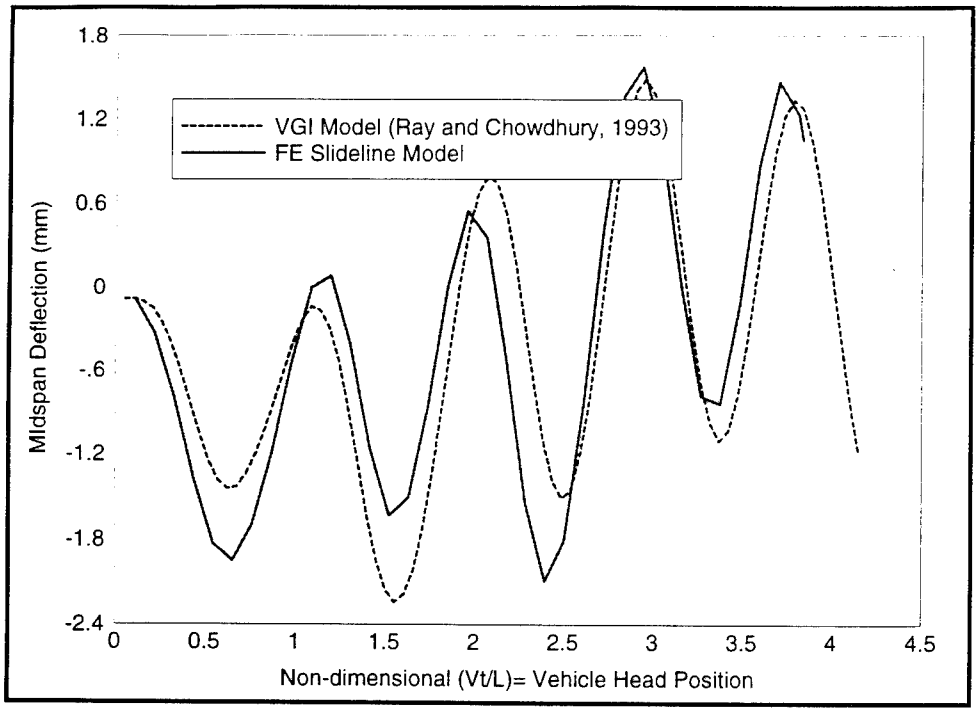

Figure 26. Comparison of analytical methodologies

Analyses Using a Simplified Guideway Mesh

FE meshes

As previously discussed, a simplified FE mesh of the Foster-Miller guideway was developed to demonstrate its applicability to VGI problems. Three different simplified meshes were developed: a single two-span guideway mesh, a multispan guideway mesh, and a curved guideway mesh. Each mesh will be discussed separately in the following paragraphs:

The two-span guideway mesh, shown in Figure 27, was a simplified version of the "Detailed Mesh" discussed in the previous section. Clarity is low in Figure 27 because it shows the actual mesh as taken directly from the FE preprocessor. Instead of shell elements (as used for the Detailed Mesh), two-noded linear beam elements were used for the simplified mesh. Rectangular cross-sections of 2 m deep by 1.3 m wide were used to represent the vertical moment of inertias (i.e., stiffnesses) of each side of the guideway. As with the Detailed Mesh, the prestressing in the guideway was applied through the pre-strained rebar elements within the beam elements.

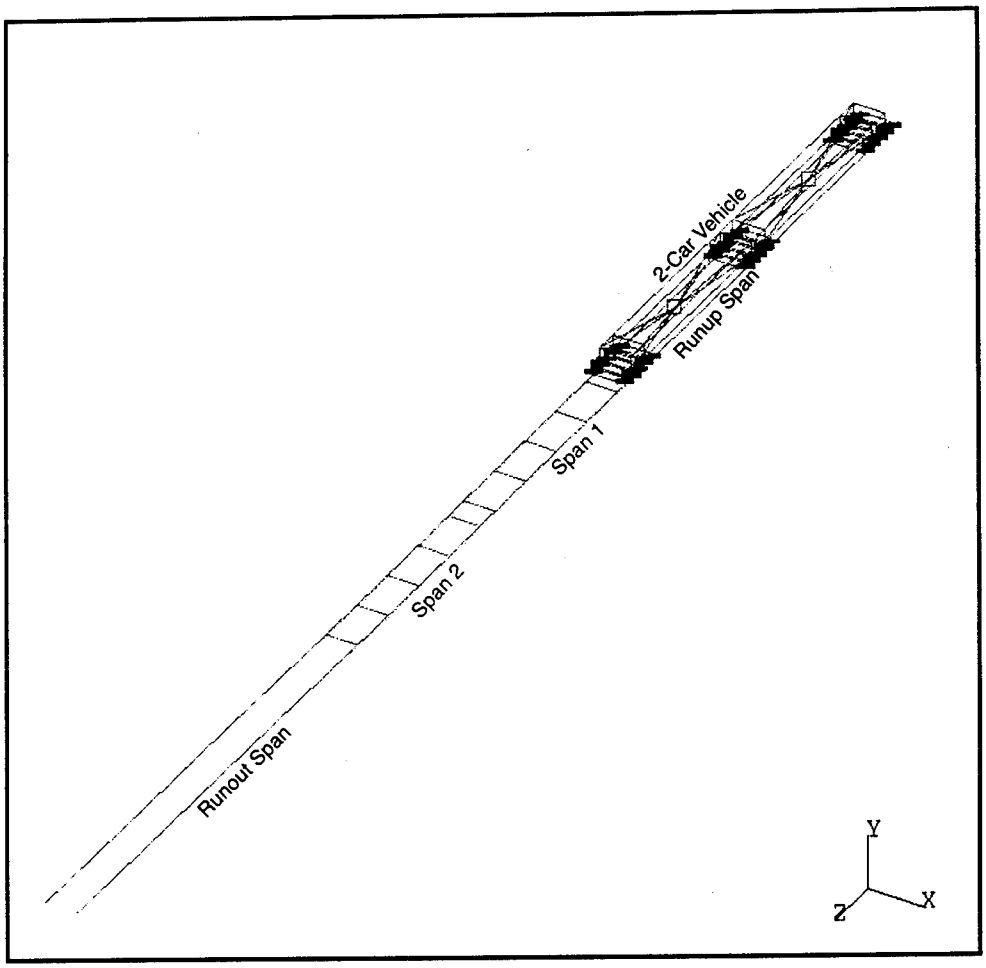

Figure 27. Two-span simplified mesh of the Foster-Miller guideway

A very important and especially difficult part of the development of the two-span mesh was matching the 3-D stiffness of the actual guideway. It was not only necessary to match the vertical stiffness of each side of the guideway, but also the combined vertical stiffness between its two sides due to the interaction of the intermediate diaphragms (Refer to Figure 15 for diaphragm details). If one side of the guideway moves downward, the diaphragms pull downward on the other side also, making the moving side actually stiffer than if it were acting alone.

For the FE mesh, the diaphragms were modeled as rectangular beam elements, rigidly connected to the guideway beam elements at the appropriate locations (approximately 4.5 m on center over the length of the guideway). The stiffness to use for the beam elements was determined through an iterative process. Equal static loads were applied to one side of both the Detailed Mesh (discussed in the previous section) and the Simplified Mesh. The stiffness of the diaphragm elements in the Simplified Mesh was varied until the resulting guideway deflections of the Simplified Mesh matched those of the Detailed Mesh. Using the same modulus of elasticity as the other beam elements in the

mesh, the resulting diaphragm element dimensions were 0.4 m deep by 0.25 m wide.

Likewise, the dynamic properties of the Simplified Mesh were calibrated to the Detailed Mesh by variation of the densities of the beam elements until the modal properties matched those of the Detailed Mesh. This process resulted in required element densities of 3.46 kg/m^3, which matched the first two vertical modes to within 5 percent and the first two lateral modes to within 25 percent.

Due to cumulative effects, vehicular ride quality will vary significantly as the vehicle moves along an infinitely long guideway. Therefore, to demonstrate the usefulness of the FE Model for ride quality analyses, a multi-span guideway mesh was developed. This was accomplished basically by extending the simplified mesh to five times its original length, to produce a total of five two-span guideways (i.e., 10 spans of 27 m each). The multispan mesh, with all the same structural properties as the previous two-span mesh, is shown in Figure 28. Again, clarity is low in this figure because it was taken directly from the FE preprocessor.

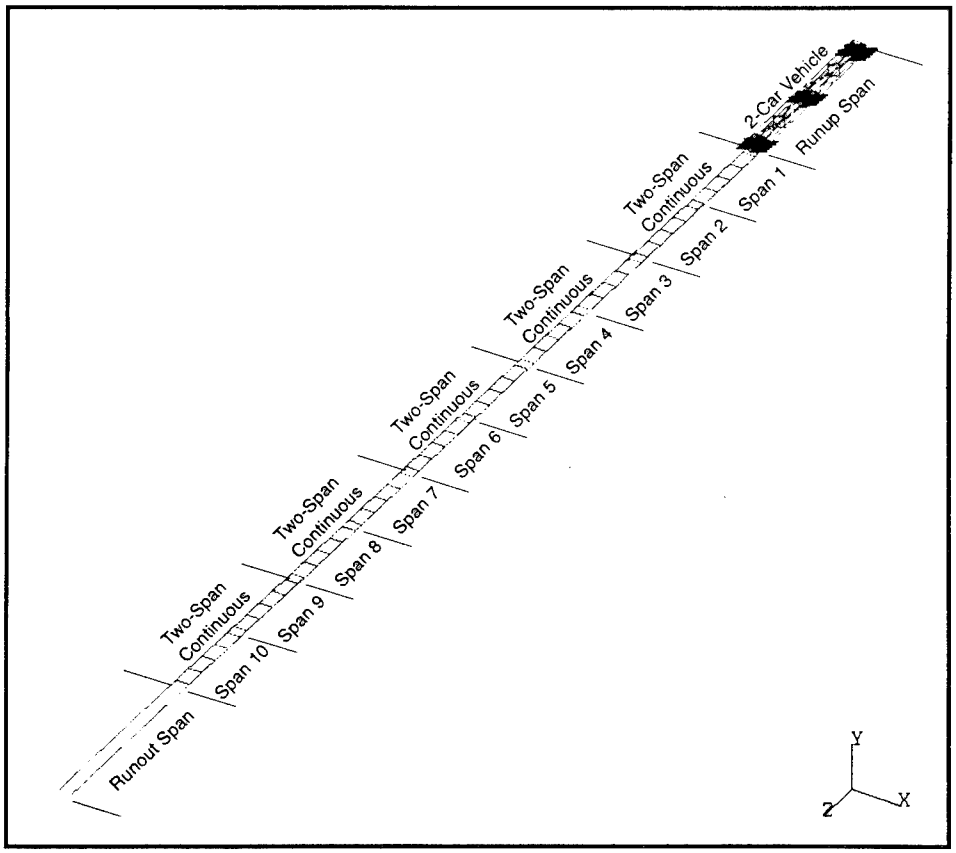

Figure 28. Ten-span simplified mesh of the Foster-Miller guideway

Ideally, more than 10 guideway spans should be used for a ride quality analysis of a system. However, it was found in this study that memory limitations on the CRAY YMP (on which these problems were run) only allowed a maximum of 350 slideline elements to be linked end-to-end. Since the element lengths were already fixed for this problem (i.e., the mesh was already generated prior to finding this problem), the number of spans were limited to 10 for the study herein. For future studies, the guideway element lengths should be optimized to allow the maximum number of spans while still accurately representing the important guideway modes.

Because of the high speeds associated with Maglev vehicles, their behavior in curves and the resulting forces on the guideway structure are an important consideration. Therefore, a curved guideway FE mesh was also developed to study the usefulness of the FE Model. A typical maglev-type curved path was modeled through an angle of 30.9 deg with a radius of 500 m. The total amount of curve that could be modeled was controlled by the previously mentioned computer memory limitation for slideline elements in a continuous path. Five consecutive two-span continuous curved spans (i.e. 10 spans total) were developed. As with the other meshed, they were connected at each end to a straight runup and runout span. The curved guideway mesh is depicted in Figure 29.

The same vehicle mesh previously described in the Detailed Mesh analysis was also used for the Simplified Mesh analyses. Similarly, slidelines were generated along each of the FE meshes to provide the sliding interaction between the vehicle and the guideway mesh.

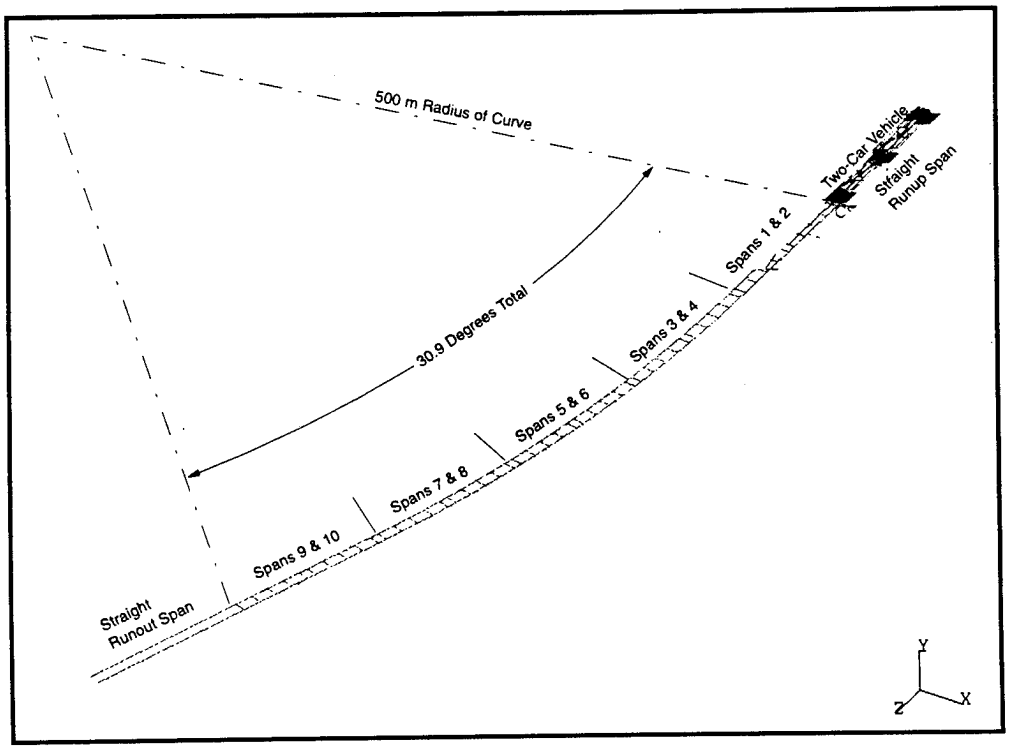

Figure 29. Curved mesh of the Foster-Miller guideway

Results

The dynamic analyses of the Simplified FE meshes described previously were also performed using the **DYNAMIC* option in the ABAQUS code and by applying a 140 mps velocity boundary condition to all of the nodes associated with the vehicle mesh. The vehicle was effectively moved across the guideway mesh at a constant forward velocity of 140 mps. The analyses were run for a total time of 0.8 sec for the 2-span guideway and 2.3 sec for the 10-span guideway in order to move the vehicle completely onto and then off of the meshes.

The dynamic response of the two-span guideway is shown in Figure 30. The curves show the deflection of the midpoints of each of the adjacent 27-m-long spans. Span 1 is the span first traversed by the vehicle. Figure 31 shows the vehicle response from this analysis compared to that of the guideway. Figures 32 and 33 compare the results from this analysis to the similar results from the Detailed Mesh analysis (previously discussed). As can be seen, the results compared very closely, indicating that the guideway was successfully simplified. The only discrepancies between the analyses are in Figure 33, beyond the head position of 2.0. This was because the runout span for the Detailed Mesh was very flexible compared to the actual guideway spans, whereas the one for the Simplified Mesh was given the same stiffness as that of the actual guideway. Therefore, the vehicle displacements for the Simplified Mesh are more accurate beyond a head position of 2.0. This discrepancy serves to point out the importance of properly modeling the stiffnesses of the runup and runout spans.

Figures 34 through 36 show the results from the 10-span analysis. Note in Figure 34 that the maximum downward response of the guideway occurred in Span 9 when the vehicle was at a head position of approximately 10.5. The maximum vehicle deflection (in Figure 36) occurred as it traversed span 5. These examples point out the importance of multiple span analyses in order to determine worst-case design parameters.

No results were obtained for the curved guideway analysis. A large effort was made to try to make the analysis run, but to no success. It was finally concluded that the relative motion of the vehicle through the curve, normal to the slideline plane (refer to Figure 6), was too great for the slideline option within ABAQUS. This was known to be a potential problem in the beginning, but it was hoped that the out-of-plane relative motions in a very large radius curve, as typical for maglev guideways, would be small enough to prevent problems. However, the problem still arose.

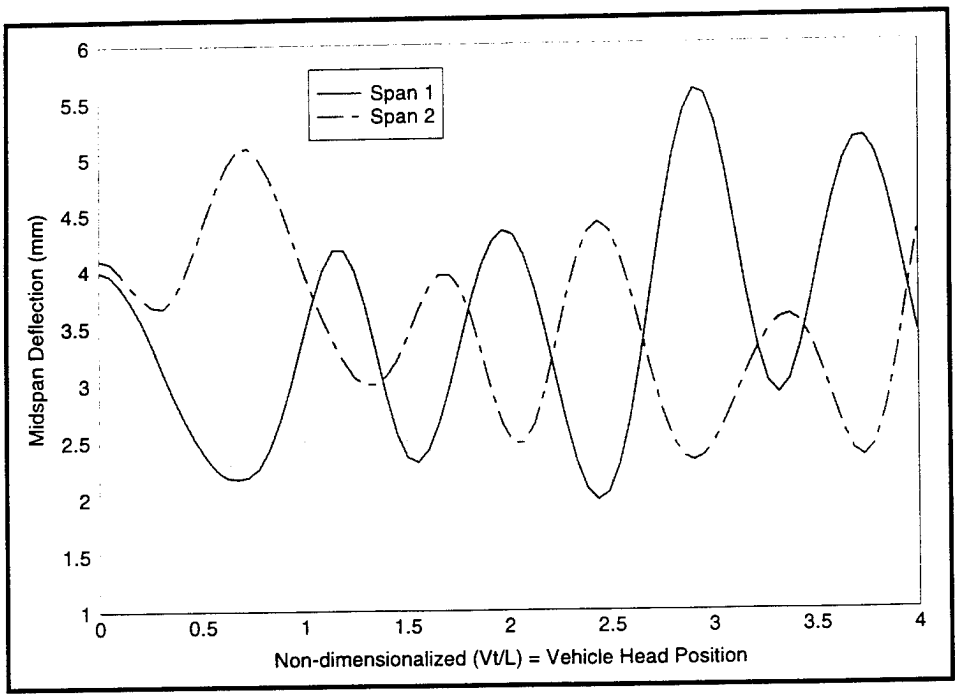

Figure 30. Midspan deflections from the two-span simplified mesh

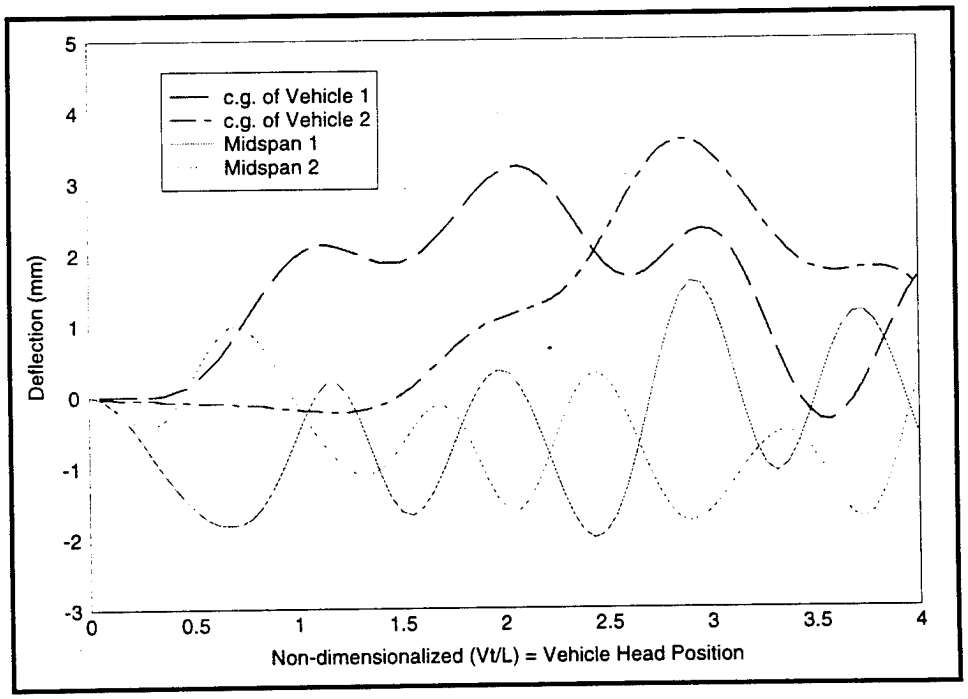

Figure 31. Comparison of vehicle and guideway deflections from the two-span simplified mesh

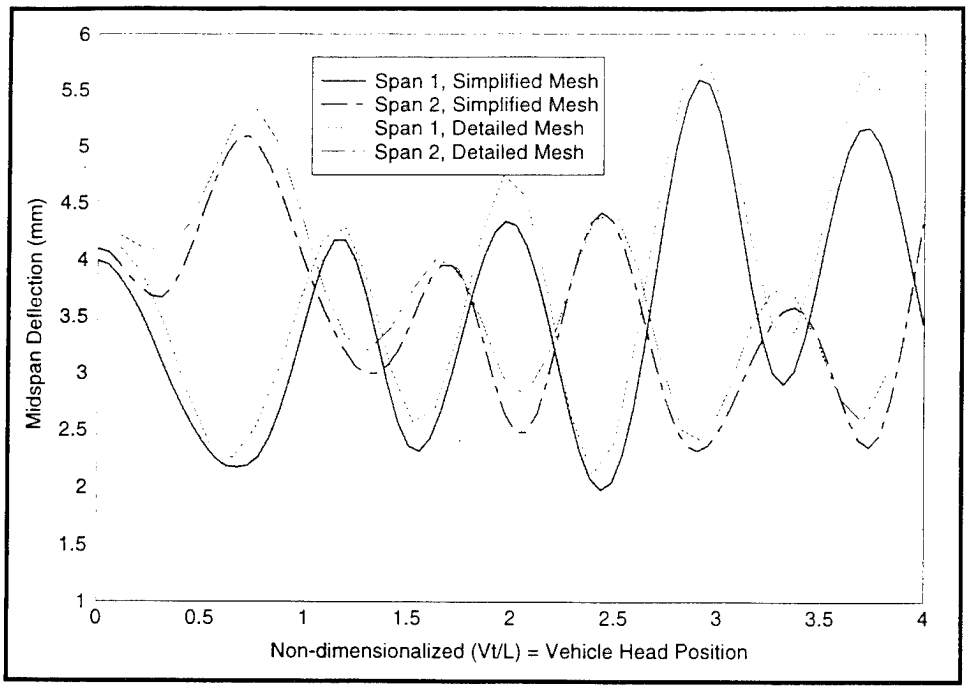

Figure 32. Comparison of guideway deflections between the Simplified Mesh and Detailed Mesh analyses

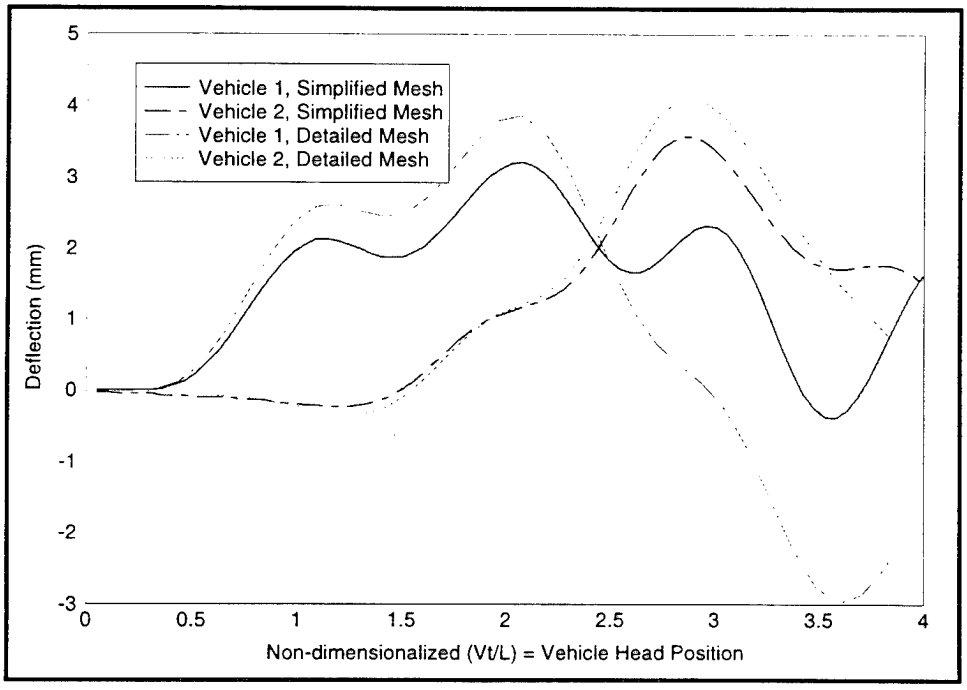

Figure 33. Comparison of vehicle deflections between the Simplified Mesh and Detailed Mesh analyses

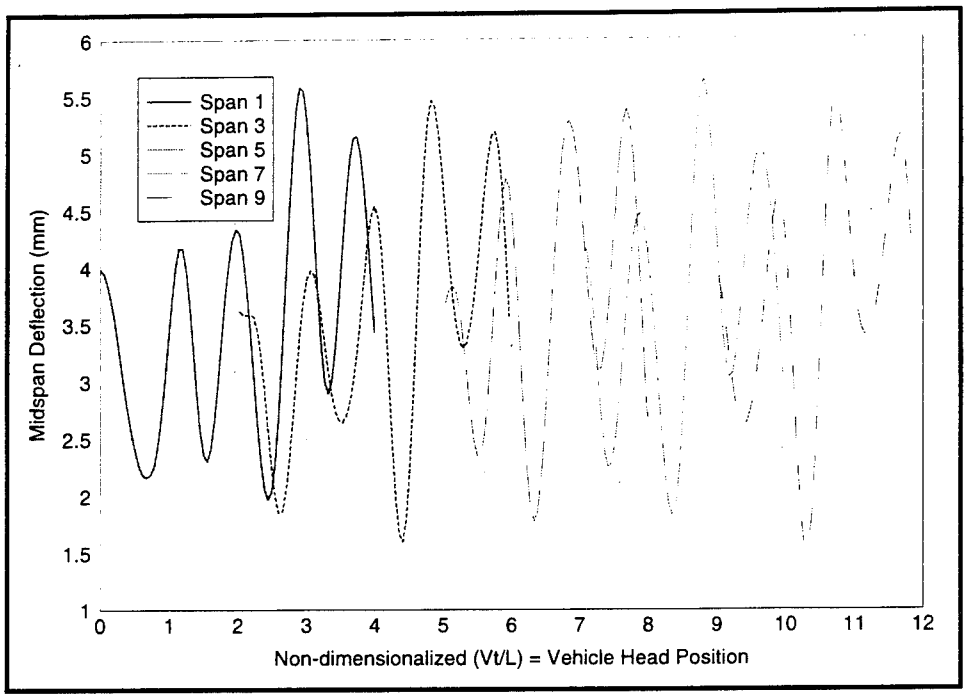

Figure 34. Midspan guideway deflections from the 10-span analysis with the simplified mesh

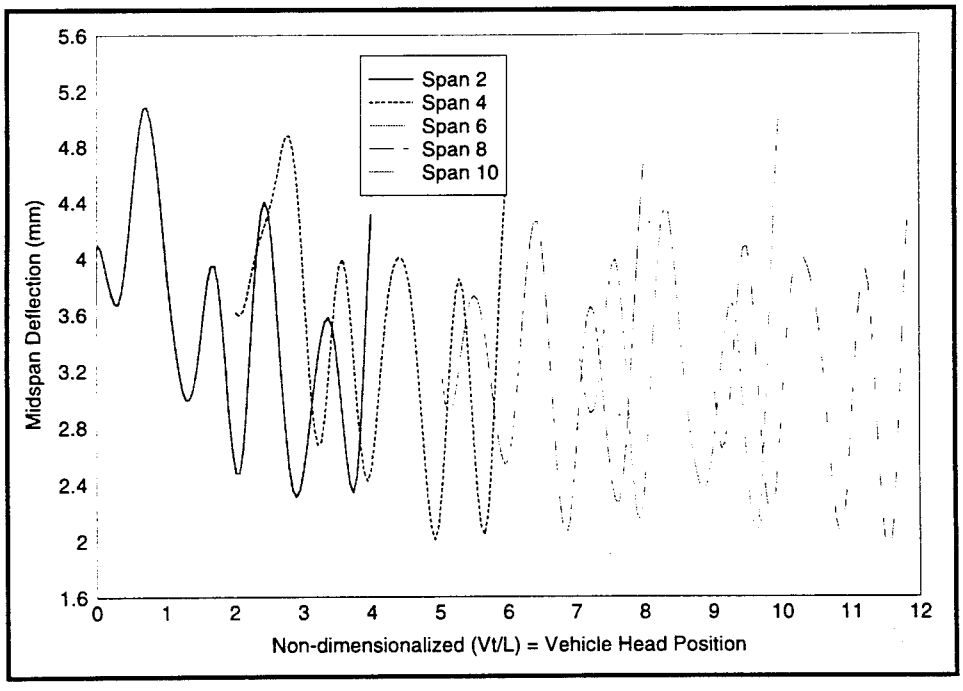

Figure 35. Midspan guideway deflections from the 10-span analysis with the simplified mesh

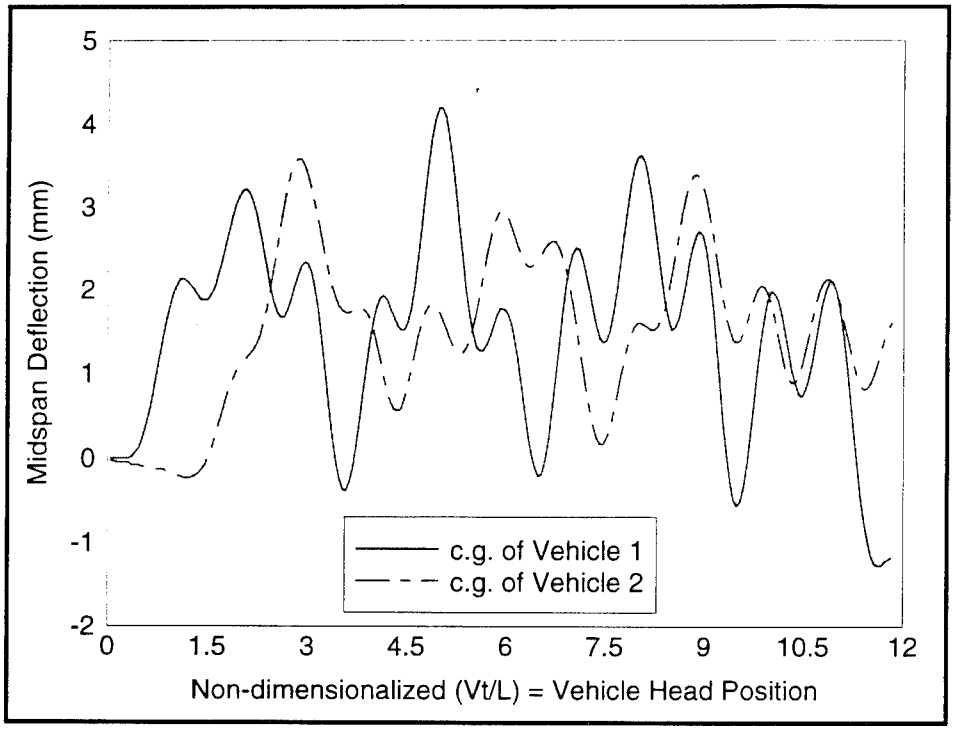

Figure 36. Vehicle deflections from the 10-span analysis with the detailed mesh

5 Conclusions and Recommendations

Conclusions

An FE Model was developed and shown to work well for the assessment of Maglev VGI. While no new FE tools were actually developed, the methodology for its application to the VGI problem was developed. Slidelines, as available in the ABAQUS code, are the key part of the Model that provide the sliding dynamic interaction between the moving vehicle and its supporting guideway. The FE Model has two distinct applications: It can be used to predict the vehicle ride quality to be expected from a given vehicle and guideway design; and to accurately predict the dynamic deflections and stresses experienced throughout a complex guideway structure as a result of a vehicle passage.

The FE Model was successfully validated in Chapter 3. The results from all three VGI analytical methods (FE solution, closed-form solution, and the VGI Model) compared very closely (refer to Figure 13). It was further validated in Chapter 4 using an actual Maglev SCD. The results from this analysis compared very closely to those from the same analysis using the VGI Model (refer to Figure 26).

The application and usefulness of the FE Model were demonstrated in Chapter 4 using the Foster-Miller SCD. It was shown that a very detailed guideway mesh can and should be used when deflections and stresses in the guideway itself are the primary concern. It was then shown how a more simplified and longer guideway mesh may be used when vehicular response is the primary concern. Because it has much fewer nodes, a much longer simplified mesh can be utilized and thus provide cumulative ride quality results as a result of a multispan traversal. However, it was found that even with a very simplified mesh, the number of slideline nodes in a row is limited due to computer memory limitations, thus limiting the total number of guideway spans depending upon the chosen FE element length. Therefore, an optimum guideway mesh will contain only the minimum number of nodes required to accurately represent the important guideway modes, thus maximizing the allowable number of guideway spans. For this reason, the FE Model will be of only limited use for in-depth vehicle ride quality analyses since these should ideally be conducted over a large number of successive guideway spans. The model is most useful as a guideway analysis tool and as a means of applying

unique 3-D vehicular loadings, such as wind effects, to the guideway.

It was found that the FE Model cannot be used on curved guideways. This limitation was attributed to the out-of-plane relative motion of the vehicle through the curve (normal to the slideline plane) being beyond that allowed by the slideline option within ABAQUS. However, while curved guideways cannot be modeled, the load effects from curves can be applied directly to the vehicle as external centrifugal forces.

In order to demonstrate the capabilities of the FE Model, a considerable effort was made herein to accurately model the Maglev vehicle and all of its response modes. It should be remembered however that strict ride quality requirements for Maglev vehicles will inherently limit vehicle movements and thus the variation in vehicular forces at the guideway level. As a result, a complete VGI analysis may not always be necessary for guideway analysis/design considerations. In many cases, movement of static vehicular gravity loadings across the guideway mesh will be sufficient for all guideway concerns. However, this assumption must be used with great care and should be applied only after careful review of the specific system under consideration.

Recommendations

Because all Maglev systems are unique and present different analytical concerns, application of the FE Model to specific problems must be done with great care and only by personnel experienced in its use. In order to gain experience in the use of this Model, future work should include its application to other Maglev systems, such as the existing German and Japanese systems and the current U.S. Maglev SCD's.

The FE Model discussed herein is currently very "code specific" in that it was developed specifically around the ABAQUS FE code. As a result, it will have limited use to those without access to and experience with these codes.

References

Foster-Miller, Inc. (1992). "Maglev System Concept Definition," Final Report, Office of Research and Development, Washington, DC.

Gallagher, R.H. (1975). *Finite Element Analysis Fundamentals.* Prentice-Hall, Inc., Englewood Cliffs, NJ.

HKS Inc. (1992). ABAQUS/Standard User's Manual, Version 5.2.

Lever, J.H. (Editor). (1993). "Technical Assessment of Maglev System Concepts, Final Report by the Government Maglev System Assessment Team," U.S. Army Cold Regions Research and Engineering Laboratory, Hanover, NH.

Meyer, C. (Editor). (1987). *Finite Element Idealization for Linear Elastic Static and Dynamic Analysis of Structures in Engineering Practice.* Task Committee on Finite Element Idealization of the Committee on Electronic Computation, Structural Division of the American Society of Civil Engineers, New York, NY.

Ray, J.C., and Chowdhury, M.R. (July 1994). "A Model for Assessment of Dynamic Interaction Between Magnetically Levitated Vehicles and Their Supporting Guideways," Technical Report SL-94-15, U.S. Army Engineer Waterways Experiment Station, Vicksburg, MS.

Richardson and Wormley. (1974). "Transportation Vehicle/Beam-Elevated Guideway Dynamic Interactions: A State-of-the-Art Review," Journal of Dynamic Systems, Measurement, and Control.

Scarborough, J.B. (1966). *Numerical Mathematical Analysis.* 6th edition, John Hopkins Press, Baltimore, MD.

Appendix A
ABAQUS Input File

```
*HEADING

This is the simplified model of the Foster-Miller
Maglev using beam elements to define the guideway.

 Units used:
  Force:  lbf
  Legth:  inch
  Time :  Sec
  Speed:  inch/sec
  Acce :  inch/sec/sec
  Mass :  lbf*sec**2/inch    =  175.16 (kg)
  Den  :  lbf*sec**2/inch**4
**
*PREPRINT, ECHO=YES, HISTORY=NO, MODEL=YES
**
*NODE, NSET=CAR_NODE
  20101,   72.1,   40.0,     0.0
  20102,   72.1,   40.0,  -100.0
  20103,   72.1,   40.0,  -924.0
  20104,   72.1,   40.0,  -1024.
  20105,   72.1,   40.0,  -1848.
  20106,   72.1,   40.0,  -1948.
  20111,   72.1,  100.0,     0.0
  20112,   72.1,  100.0,  -100.0
  20113,   72.1,  100.0,  -924.0
  20114,   72.1,  100.0,  -1024.
  20115,   72.1,  100.0,  -1848.
  20116,   72.1,  100.0,  -1948.
  20201,  -72.1,   40.0,     0.0
  20202,  -72.1,   40.0,  -100.0
  20203,  -72.1,   40.0,  -924.0
  20204,  -72.1,   40.0,  -1024.
  20205,  -72.1,   40.0,  -1848.
  20206,  -72.1,   40.0,  -1948.
  20211,  -72.1,  100.0,     0.0
  20212,  -72.1,  100.0,  -100.0
  20213,  -72.1,  100.0,  -924.0
```

```
  20214, -72.1, 100.0,  -1024.
  20215, -72.1, 100.0,  -1848.
  20216, -72.1, 100.0,  -1948.
*ELEMENT, TYPE=C3D8, ELSET=E_CAR
  20101,  20201, 20202, 20212, 20211,  20101, 20102,
20112, 20111
  20102,  20202, 20203, 20213, 20212,  20102, 20103,
20113, 20112
  20104,  20204, 20205, 20215, 20214,  20104, 20105,
20115, 20114
  20105,  20205, 20206, 20216, 20215,  20105, 20106,
20116, 20115
*SOLID SECTION, ELSET=E_CAR, MATERIAL=M_V
*MATERIAL, NAME=M_V
*ELASTIC
 30E6, 0.0
*DENSITY
 1.6149E-5,
** 1E-10,
*NSET, NSET=N_F_L, GENERATE
 21131, 21135, 1
 20131, 20134, 1
*NSET, NSET=N_F_R, GENERATE
 21231, 21235, 1
 20231, 20234, 1
*NSET, NSET=N_M_L, GENERATE
 21141, 21145, 1
 20141, 20144, 1
*NSET, NSET=N_M_R, GENERATE
 21241, 21245, 1
 20241, 20244, 1
*NSET, NSET=N_R_L, GENERATE
 21151, 21155, 1
 20151, 20154, 1
*NSET, NSET=N_R_R, GENERATE
 21251, 21255, 1
 20251, 20254, 1
*EQUATION
  2,
 N_F_L, 1, 1.0, 20135, 1, -1.0
  2,
 N_F_R, 1, 1.0, 20235, 1, -1.0
  2,
 N_M_L, 1, 1.0, 20145, 1, -1.0
  2,
 N_M_R, 1, 1.0, 20245, 1, -1.0
  2,
 N_R_L, 1, 1.0, 20155, 1, -1.0
  2,
 N_R_R, 1, 1.0, 20255, 1, -1.0
```

```
*NODE, NSET=CAR_CENT
 20100,   0.0, 40, -462.0
 20200,   0.0, 40, -1486.
**   *ELEMENT, TYPE=MASS, ELSET=CAR_MASS
**    20100,  20100
**    20200,  20200
**   *MASS, ELSET=CAR_MASS
**   ************************ 129.1 lbf*sec**2/inch =
22630 kgm
**    129.1,
*ELEMENT, TYPE=ROTARYI, ELSET=CAR_ROTA
 21100,  20100
 21200,  20200
*ROTARY INERTIA, ELSET=CAR_ROTA
************************ 21.935E6 inch**2-
lbf*sec**2/inch = 2.48E6 kgm-m**2
 21.935E6,
**   *MPC
*ELEMENT, TYPE=B31, ELSET=LINK
 29101, 20101, 20100
 29103, 20103, 20100
 29201, 20201, 20100
 29203, 20203, 20100
 29111, 20111, 20100
 29113, 20113, 20100
 29211, 20211, 20100
 29213, 20213, 20100
 29104, 20104, 20200
 29106, 20106, 20200
 29204, 20204, 20200
 29206, 20206, 20200
 29114, 20114, 20200
 29116, 20116, 20200
 29214, 20214, 20200
 29216, 20216, 20200
*BEAM SECTION, SECT=RECT, MATERIAL=M_BOGIE, ELSET=LINK
  2.50, 4.00
  1.0,0.0,0.0
*NODE, NSET=N_BOGIE
** following is for front bogie
 20131,  72.1, 30.315,  50.0
 20132,  72.1, 30.315,   0.0
 20133,  72.1, 30.315, -50.0
 20134,  72.1, 30.315, -100.
 20135,  72.1, 30.315, -150.
 20231, -72.1, 30.315,  50.0
 20232, -72.1, 30.315,   0.0
 20233, -72.1, 30.315, -50.0
 20234, -72.1, 30.315, -100.
 20235, -72.1, 30.315, -150.
```

```
** following is for middle bogie
 20141,  72.1, 30.315,  -874
 20142,  72.1, 30.315,  -924
 20143,  72.1, 30.315,  -974
 20144,  72.1, 30.315, -1024
 20145,  72.1, 30.315, -1074
 20241, -72.1, 30.315,  -874
 20242, -72.1, 30.315,  -924
 20243, -72.1, 30.315,  -974
 20244, -72.1, 30.315, -1024
 20245, -72.1, 30.315, -1074
** following is for rear bogie
 20151,  72.1, 30.315,  -1798
 20152,  72.1, 30.315,  -1848
 20153,  72.1, 30.315,  -1898
 20154,  72.1, 30.315,  -1948
 20155,  72.1, 30.315,  -1998
 20251, -72.1, 30.315,  -1798
 20252, -72.1, 30.315,  -1848
 20253, -72.1, 30.315,  -1898
 20254, -72.1, 30.315,  -1948
 20255, -72.1, 30.315,  -1998
*ELEMENT, TYPE=B31, ELSET=ENDBOGIE
** front bogie
 20131, 20131, 20132
 20132, 20132, 20133
 20133, 20133, 20134
 20134, 20134, 20135
 20231, 20231, 20232
 20232, 20232, 20233
 20233, 20233, 20234
 20234, 20234, 20235
** rear bogie
 20151, 20151, 20152
 20152, 20152, 20153
 20153, 20153, 20154
 20154, 20154, 20155
 20251, 20251, 20252
 20252, 20252, 20253
 20253, 20253, 20254
 20254, 20254, 20255
*BEAM SECTION, SECT=RECT, MATERIAL=M_BOGIE,
ELSET=ENDBOGIE
 25.0, 40.0
 1.0,0.0,0.0
*ELEMENT, TYPE=B31, ELSET=MIDBOGIE
 20141, 20141, 20142
 20142, 20142, 20143
 20143, 20143, 20144
 20144, 20144, 20145
 20241, 20241, 20242
 20242, 20242, 20243
 20243, 20243, 20244
```

```
 20244, 20244, 20245
*BEAM SECTION, SECT=RECT, MATERIAL=M_BOGIE,
ELSET=MIDBOGIE
******** --> use different beam cross-sections to
reflect bogie mass difference
 30.0, 40.0
 1.0,0.0,0.0
*MATERIAL, NAME=M_BOGIE
*ELASTIC
 30E6, 0.0
***** DENSITY IS SO CALCULATED THAT TOTAL MASS = MASS
IN 2 BOGIES
*DENSITY
********** -->  each bogie volume = 200x40x25 = 2E5
inch**3
********** -->  Mass = 2E5x8.745E-5 = 17.49
lbf*sec**2/inch = 3065 kgm
 8.745E-5,
*NCOPY, OLD SET=N_BOGIE, NEW SET=N_ISL, CHANGE
NUMBER=1000, SHIFT
 0.0, -30.315, 0.0

*ELEMENT, TYPE=C3D8, ELSET=CHASIS
 30001, 21231, 21232, 20232, 20231, 21131, 21132,
20132, 20131
 30011, 21241, 21242, 20242, 20241, 21141, 21142,
20142, 20141
 30021, 21251, 21252, 20252, 20251, 21151, 21152,
20152, 20151
 30101, 20232, 20234, 20202, 20201, 20132, 20134,
20102, 20101
 30102, 20242, 20244, 20204, 20203, 20142, 20144,
20104, 20103
 30103, 20252, 20254, 20206, 20205, 20152, 20154,
20106, 20105
 30201, 20203, 20204, 20214, 20213, 20103, 20104,
20114, 20113
*ELGEN, ELSET=CHASIS
 30001, 4, 1, 1
 30011, 4, 1, 1
 30021, 4, 1, 1
*SOLID SECTION, ELSET=CHASIS, MATERIAL=M_CHASIS
*MATERIAL, NAME=M_CHASIS
*ELASTIC
 10., 0.0
** 10E3, 0.0
*DENSITY
 1E-10,
*ELEMENT, TYPE=ISL31, ELSET=SLIDE
** front slide
 21131, 21131, 21132
 21132, 21132, 21133
 21133, 21133, 21134
```

```
 21134, 21134, 21135
 21231, 21231, 21232
 21232, 21232, 21233
 21233, 21233, 21234
 21234, 21234, 21235
** middle slide
 21141, 21141, 21142
 21142, 21142, 21143
 21143, 21143, 21144
 21144, 21144, 21145
 21241, 21241, 21242
 21242, 21242, 21243
 21243, 21243, 21244
 21244, 21244, 21245
** rear slide
 21151, 21151, 21152
 21152, 21152, 21153
 21153, 21153, 21154
 21154, 21154, 21155
 21251, 21251, 21252
 21252, 21252, 21253
 21253, 21253, 21254
 21254, 21254, 21255
*ELSET, ELSET=MAG_L, GENERATE
 21131, 21154, 1
*INTERFACE, ELSET=MAG_L
 1.0,  -1.0,-1.0,0.0
*SURFACE CONTACT, NO SEPARATION
*SLIDE LINE, TYPE=LINEAR, SMOOTH=.2, ELSET=MAG_L,
GENERATE
10019, 10019,  0
   19,    75, 56
  133,   413, 56
  471,   751, 56
  809,  1089, 56
 1147,  1427, 56
 1485,  1545, 60
 1603,  1661, 58
 1717,  1941, 56
 1999,  2279, 56
 2337,  2617, 56
 2675,  2955, 56
 3013,  3073, 60
13073, 13073,  0
*ELSET, ELSET=MAG_R, GENERATE
 21231, 21254, 1
*INTERFACE, ELSET=MAG_R
 1.0,  -1.0,1.0,0.0
*SURFACE CONTACT, NO SEPARATION
*SLIDE LINE, TYPE=LINEAR, SMOOTH=.2, ELSET=MAG_R,
GENERATE
10010, 10010, 0
   10,    66, 56
```

```
  124,   404, 56
  462,   742, 56
  800,  1080, 56
 1138,  1418, 56
 1476,  1534, 58
 1594,  1652, 58
 1708,  1932, 56
 1990,  2270, 56
 2328,  2608, 56
 2666,  2946, 56
 3004,  3062, 58
13062, 13062, 0
**
*** use springs to represent suspensions
*ELEMENT, TYPE=SPRINGA, ELSET=SUSPEN_P
** front suspension
 22131, 20131, 21131
 22132, 20132, 21132
 22133, 20133, 21133
 22134, 20134, 21134
 22135, 20135, 21135
 22231, 20231, 21231
 22232, 20232, 21232
 22233, 20233, 21233
 22234, 20234, 21234
 22235, 20235, 21235
** middle suspension
 22141, 20141, 21141
 22142, 20142, 21142
 22143, 20143, 21143
 22144, 20144, 21144
 22145, 20145, 21145
 22241, 20241, 21241
 22242, 20242, 21242
 22243, 20243, 21243
 22244, 20244, 21244
 22245, 20245, 21245
** rear suspension
 22151, 20151, 21151
 22152, 20152, 21152
 22153, 20153, 21153
 22154, 20154, 21154
 22155, 20155, 21155
 22251, 20251, 21251
 22252, 20252, 21252
 22253, 20253, 21253
 22254, 20254, 21254
 22255, 20255, 21255
*SPRING, ELSET=SUSPEN_P
1513.4,
***************** 10 x 1513.4 lbf/inch = 2.651E6 N/m
```

```
*ELEMENT, TYPE=SPRINGA, ELSET=SUS_S_E
 23101, 20101, 20132
 23102, 20102, 20134
 23105, 20105, 20152
 23106, 20106, 20154
 23201, 20201, 20232
 23202, 20202, 20234
 23205, 20205, 20252
 23206, 20206, 20254
*SPRING, ELSET=SUS_S_E

 1712.7,
****************** 4 x 1712.7 lbf/inch = 1.2E6 N/m
*ELEMENT, TYPE=SPRINGA, ELSET=SUS_S_M
 23103, 20103, 20142
 23104, 20104, 20144
 23203, 20203, 20242
 23204, 20204, 20244
*SPRING, ELSET=SUS_S_M

 856.4,
****************** 4 x 856.4 lbf/inch = 0.6E6 N/m
**
*** use truss for illustration
**
*ELEMENT, TYPE=C1D2, ELSET=TRUSS
** front suspension
 24131, 20131, 21131
 24132, 20132, 21132
 24133, 20133, 21133
 24134, 20134, 21134
 24135, 20135, 21135
 24231, 20231, 21231
 24232, 20232, 21232
 24233, 20233, 21233
 24234, 20234, 21234
 24235, 20235, 21235
** middle suspension
 24141, 20141, 21141
 24142, 20142, 21142
 24143, 20143, 21143
 24144, 20144, 21144
 24145, 20145, 21145
 24241, 20241, 21241
 24242, 20242, 21242
 24243, 20243, 21243
 24244, 20244, 21244
 24245, 20245, 21245
** rear suspension
 24151, 20151, 21151
 24152, 20152, 21152
 24153, 20153, 21153
 24154, 20154, 21154
```

```
 24155, 20155, 21155
 24251, 20251, 21251
 24252, 20252, 21252
 24253, 20253, 21253
 24254, 20254, 21254
 24255, 20255, 21255
** secondary suspensions
 25101, 20101, 20132
 25102, 20102, 20134
 25103, 20103, 20142
 25104, 20104, 20144
 25105, 20105, 20152
 25106, 20106, 20154
 25201, 20201, 20232
 25202, 20202, 20234
 25203, 20203, 20242
 25204, 20204, 20244
 25205, 20205, 20252
 25206, 20206, 20254
*SOLID SECTION, ELSET=TRUSS, MATERIAL=M_V
 1E-6,
*ELEMENT, TYPE=DASHPOTA, ELSET=DASHPOT
 26101, 20101, 20132
 26102, 20102, 20134
 26103, 20103, 20142
 26104, 20104, 20144
 26105, 20105, 20152
 26106, 20106, 20154
 26201, 20201, 20232
 26202, 20202, 20234
 26203, 20203, 20242
 26204, 20204, 20244
 26205, 20205, 20252
 26206, 20206, 20254
*DASHPOT, ELSET=DASHPOT

************************* 2 X 14.25 lbf*s/inch = 0.5E4
N*s/m
 14.25,
*NSET, NSET=VEHICLE
** N_ISL, CAR_CENT, CAR_NODE,
 N_ISL, N_BOGIE, CAR_CENT, CAR_NODE,
*ELSET, ELSET=V_MASS
 ENDBOGIE, MIDBOGIE
*ELSET, ELSET=CARFRAME
 E_CAR, ENDBOGIE, MIDBOGIE, SLIDE, TRUSS
*NMAP, TYPE=RECTANGULAR, NSET=VEHICLE
 0.0, 0.0, -50.0

 1.0, 1.0, 1.0
*NODE, SYSTEM=R, NSET=ENDNODES
      10019, 7.2091E+01, 0.0000E+00, -2100.0000E+00
      10010,-7.2091E+01, 0.0000E+00, -2100.0000E+00
```

```
      13062,-7.2091E+01, 0.0000E+00, 4.2260E+03
      13073, 7.2091E+01, 0.0000E+00, 4.2260E+03
*NSET, NSET=NTRACK, GENE
10019, 10019,  0
   19,    75, 56
  133,   413, 56
  471,   751, 56
  809,  1089, 56
 1147,  1427, 56
 1485,  1545, 60
 1603,  1661, 58
 1717,  1941, 56
 1999,  2279, 56
 2337,  2617, 56
 2675,  2955, 56
 3013,  3073, 60
13073, 13073,  0
**
10010, 10010, 0
   10,    66, 56
  124,   404, 56
  462,   742, 56
  800,  1080, 56
 1138,  1418, 56
 1476,  1534, 58
 1594,  1652, 58
 1708,  1932, 56
 1990,  2270, 56
 2328,  2608, 56
 2666,  2946, 56
 3004,  3062, 58
13062, 13062, 0
*ELEMENT, TYPE=B31, ELSET=ENDTRACK
  10019, 10019,    19
  10010, 10010,    10
  13062, 13062,  3062
  13073, 13073,  3073
*BEAM SECTION, SECT=RECT, MATERIAL=M_END,
ELSET=ENDTRACK
 5.0, 10.0
 1.0,0.0,0.0
*MATERIAL, NAME=M_END
*ELASTIC
 30E6, 0.3
*DENSITY
 1E-6,
**
```

```
**************************************************
** These nodes will be used for the definition     *
** of the beam elements of the guideway. They are *
** the same as used to define the slidelines.     *
**************************************************
**
*NODE, SYSTEM=R,NSET=RIGHT
**
         10,-7.2091E+01, 0.0000E+00, 0.0000E+00
         38,-7.2091E+01, 0.0000E+00, 1.9685E+01
         66,-7.2091E+01, 0.0000E+00, 3.9370E+01
         94,-7.2091E+01, 0.0000E+00, 5.9055E+01
        124,-7.2091E+01, 0.0000E+00, 7.8740E+01
        152,-7.2091E+01, 0.0000E+00, 9.8425E+01
        180,-7.2091E+01, 0.0000E+00, 1.1811E+02
        208,-7.2091E+01, 0.0000E+00, 1.3780E+02
        236,-7.2091E+01, 0.0000E+00, 1.5748E+02
        264,-7.2091E+01, 0.0000E+00, 1.7717E+02
        292,-7.2091E+01, 0.0000E+00, 1.9685E+02
        320,-7.2091E+01, 0.0000E+00, 2.1654E+02
        348,-7.2091E+01, 0.0000E+00, 2.3622E+02
        376,-7.2091E+01, 0.0000E+00, 2.5591E+02
        404,-7.2091E+01, 0.0000E+00, 2.7559E+02
        432,-7.2091E+01, 0.0000E+00, 2.9528E+02
        462,-7.2091E+01, 0.0000E+00, 3.1496E+02
        490,-7.2091E+01, 0.0000E+00, 3.3465E+02
        518,-7.2091E+01, 0.0000E+00, 3.5433E+02
        546,-7.2091E+01, 0.0000E+00, 3.7402E+02
        574,-7.2091E+01, 0.0000E+00, 3.9370E+02
        602,-7.2091E+01, 0.0000E+00, 4.1339E+02
        630,-7.2091E+01, 0.0000E+00, 4.3307E+02
        658,-7.2091E+01, 0.0000E+00, 4.5276E+02
        686,-7.2091E+01, 0.0000E+00, 4.7244E+02
        714,-7.2091E+01, 0.0000E+00, 4.9213E+02
        742,-7.2091E+01, 0.0000E+00, 5.1181E+02
        770,-7.2091E+01, 0.0000E+00, 5.3150E+02
        800,-7.2091E+01, 0.0000E+00, 5.5118E+02
        828,-7.2091E+01, 0.0000E+00, 5.7087E+02
        856,-7.2091E+01, 0.0000E+00, 5.9055E+02
        884,-7.2091E+01, 0.0000E+00, 6.1024E+02
        912,-7.2091E+01, 0.0000E+00, 6.2992E+02
        940,-7.2091E+01, 0.0000E+00, 6.4961E+02
        968,-7.2091E+01, 0.0000E+00, 6.6929E+02
        996,-7.2091E+01, 0.0000E+00, 6.8898E+02
       1024,-7.2091E+01, 0.0000E+00, 7.0866E+02
       1052,-7.2091E+01, 0.0000E+00, 7.2835E+02
       1080,-7.2091E+01, 0.0000E+00, 7.4803E+02
       1108,-7.2091E+01, 0.0000E+00, 7.6772E+02
       1138,-7.2091E+01, 0.0000E+00, 7.8740E+02
       1166,-7.2091E+01, 0.0000E+00, 8.0709E+02
       1194,-7.2091E+01, 0.0000E+00, 8.2677E+02
       1222,-7.2091E+01, 0.0000E+00, 8.4646E+02
       1250,-7.2091E+01, 0.0000E+00, 8.6614E+02
```

```
1278,-7.2091E+01, 0.0000E+00, 8.8583E+02
1306,-7.2091E+01, 0.0000E+00, 9.0551E+02
1334,-7.2091E+01, 0.0000E+00, 9.2520E+02
1362,-7.2091E+01, 0.0000E+00, 9.4488E+02
1390,-7.2091E+01, 0.0000E+00, 9.6457E+02
1418,-7.2091E+01, 0.0000E+00, 9.8425E+02
1446,-7.2091E+01, 0.0000E+00, 1.0039E+03
1476,-7.2091E+01, 0.0000E+00, 1.0236E+03
1504,-7.2091E+01, 0.0000E+00, 1.0433E+03
1534,-7.2091E+01, 0.0000E+00, 1.0630E+03
1566,-7.2091E+01, 0.0000E+00, 1.0827E+03
1594,-7.2091E+01, 0.0000E+00, 1.1024E+03
1622,-7.2091E+01, 0.0000E+00, 1.1220E+03
1652,-7.2091E+01, 0.0000E+00, 1.1417E+03
1680,-7.2091E+01, 0.0000E+00, 1.1614E+03
1708,-7.2091E+01, 0.0000E+00, 1.1811E+03
1736,-7.2091E+01, 0.0000E+00, 1.2008E+03
1764,-7.2091E+01, 0.0000E+00, 1.2205E+03
1792,-7.2091E+01, 0.0000E+00, 1.2402E+03
1820,-7.2091E+01, 0.0000E+00, 1.2598E+03
1848,-7.2091E+01, 0.0000E+00, 1.2795E+03
1876,-7.2091E+01, 0.0000E+00, 1.2992E+03
1904,-7.2091E+01, 0.0000E+00, 1.3189E+03
1932,-7.2091E+01, 0.0000E+00, 1.3386E+03
1960,-7.2091E+01, 0.0000E+00, 1.3583E+03
1990,-7.2091E+01, 0.0000E+00, 1.3780E+03
2018,-7.2091E+01, 0.0000E+00, 1.3976E+03
2046,-7.2091E+01, 0.0000E+00, 1.4173E+03
2074,-7.2091E+01, 0.0000E+00, 1.4370E+03
2102,-7.2091E+01, 0.0000E+00, 1.4567E+03
2130,-7.2091E+01, 0.0000E+00, 1.4764E+03
2158,-7.2091E+01, 0.0000E+00, 1.4961E+03
2186,-7.2091E+01, 0.0000E+00, 1.5157E+03
2214,-7.2091E+01, 0.0000E+00, 1.5354E+03
2242,-7.2091E+01, 0.0000E+00, 1.5551E+03
2270,-7.2091E+01, 0.0000E+00, 1.5748E+03
2298,-7.2091E+01, 0.0000E+00, 1.5945E+03
2328,-7.2091E+01, 0.0000E+00, 1.6142E+03
2356,-7.2091E+01, 0.0000E+00, 1.6339E+03
2384,-7.2091E+01, 0.0000E+00, 1.6535E+03
2412,-7.2091E+01, 0.0000E+00, 1.6732E+03
2440,-7.2091E+01, 0.0000E+00, 1.6929E+03
2468,-7.2091E+01, 0.0000E+00, 1.7126E+03
2496,-7.2091E+01, 0.0000E+00, 1.7323E+03
2524,-7.2091E+01, 0.0000E+00, 1.7520E+03
2552,-7.2091E+01, 0.0000E+00, 1.7717E+03
2580,-7.2091E+01, 0.0000E+00, 1.7913E+03
2608,-7.2091E+01, 0.0000E+00, 1.8110E+03
2636,-7.2091E+01, 0.0000E+00, 1.8307E+03
2666,-7.2091E+01, 0.0000E+00, 1.8504E+03
2694,-7.2091E+01, 0.0000E+00, 1.8701E+03
2722,-7.2091E+01, 0.0000E+00, 1.8898E+03
2750,-7.2091E+01, 0.0000E+00, 1.9094E+03
```

```
2778,-7.2091E+01, 0.0000E+00, 1.9291E+03
2806,-7.2091E+01, 0.0000E+00, 1.9488E+03
2834,-7.2091E+01, 0.0000E+00, 1.9685E+03
2862,-7.2091E+01, 0.0000E+00, 1.9882E+03
2890,-7.2091E+01, 0.0000E+00, 2.0079E+03
2918,-7.2091E+01, 0.0000E+00, 2.0276E+03
2946,-7.2091E+01, 0.0000E+00, 2.0472E+03
2974,-7.2091E+01, 0.0000E+00, 2.0669E+03
3004,-7.2091E+01, 0.0000E+00, 2.0866E+03
3032,-7.2091E+01, 0.0000E+00, 2.1063E+03
3062,-7.2091E+01, 0.0000E+00, 2.1260E+03
**
*NODE, SYSTEM=R,NSET=LEFT
**
  19, 7.2091E+01, 0.0000E+00, 0.0000E+00
  47, 7.2091E+01, 0.0000E+00, 1.9685E+01
  75, 7.2091E+01, 0.0000E+00, 3.9370E+01
 105, 7.2091E+01, 0.0000E+00, 5.9055E+01
 133, 7.2091E+01, 0.0000E+00, 7.8740E+01
 161, 7.2091E+01, 0.0000E+00, 9.8425E+01
 189, 7.2091E+01, 0.0000E+00, 1.1811E+02
 217, 7.2091E+01, 0.0000E+00, 1.3780E+02
 245, 7.2091E+01, 0.0000E+00, 1.5748E+02
 273, 7.2091E+01, 0.0000E+00, 1.7717E+02
 301, 7.2091E+01, 0.0000E+00, 1.9685E+02
 329, 7.2091E+01, 0.0000E+00, 2.1654E+02
 357, 7.2091E+01, 0.0000E+00, 2.3622E+02
 385, 7.2091E+01, 0.0000E+00, 2.5591E+02
 413, 7.2091E+01, 0.0000E+00, 2.7559E+02
 443, 7.2091E+01, 0.0000E+00, 2.9528E+02
 471, 7.2091E+01, 0.0000E+00, 3.1496E+02
 499, 7.2091E+01, 0.0000E+00, 3.3465E+02
 527, 7.2091E+01, 0.0000E+00, 3.5433E+02
 555, 7.2091E+01, 0.0000E+00, 3.7402E+02
 583, 7.2091E+01, 0.0000E+00, 3.9370E+02
 611, 7.2091E+01, 0.0000E+00, 4.1339E+02
 639, 7.2091E+01, 0.0000E+00, 4.3307E+02
 667, 7.2091E+01, 0.0000E+00, 4.5276E+02
 695, 7.2091E+01, 0.0000E+00, 4.7244E+02
 723, 7.2091E+01, 0.0000E+00, 4.9213E+02
 751, 7.2091E+01, 0.0000E+00, 5.1181E+02
 781, 7.2091E+01, 0.0000E+00, 5.3150E+02
 809, 7.2091E+01, 0.0000E+00, 5.5118E+02
 837, 7.2091E+01, 0.0000E+00, 5.7087E+02
 865, 7.2091E+01, 0.0000E+00, 5.9055E+02
 893, 7.2091E+01, 0.0000E+00, 6.1024E+02
 921, 7.2091E+01, 0.0000E+00, 6.2992E+02
 949, 7.2091E+01, 0.0000E+00, 6.4961E+02
 977, 7.2091E+01, 0.0000E+00, 6.6929E+02
1005, 7.2091E+01, 0.0000E+00, 6.8898E+02
1033, 7.2091E+01, 0.0000E+00, 7.0866E+02
1061, 7.2091E+01, 0.0000E+00, 7.2835E+02
1089, 7.2091E+01, 0.0000E+00, 7.4803E+02
```

```
1119, 7.2091E+01, 0.0000E+00, 7.6772E+02
1147, 7.2091E+01, 0.0000E+00, 7.8740E+02
1175, 7.2091E+01, 0.0000E+00, 8.0709E+02
1203, 7.2091E+01, 0.0000E+00, 8.2677E+02
1231, 7.2091E+01, 0.0000E+00, 8.4646E+02
1259, 7.2091E+01, 0.0000E+00, 8.6614E+02
1287, 7.2091E+01, 0.0000E+00, 8.8583E+02
1315, 7.2091E+01, 0.0000E+00, 9.0551E+02
1343, 7.2091E+01, 0.0000E+00, 9.2520E+02
1371, 7.2091E+01, 0.0000E+00, 9.4488E+02
1399, 7.2091E+01, 0.0000E+00, 9.6457E+02
1427, 7.2091E+01, 0.0000E+00, 9.8425E+02
1457, 7.2091E+01, 0.0000E+00, 1.0039E+03
1485, 7.2091E+01, 0.0000E+00, 1.0236E+03
1513, 7.2091E+01, 0.0000E+00, 1.0433E+03
1545, 7.2091E+01, 0.0000E+00, 1.0630E+03
1575, 7.2091E+01, 0.0000E+00, 1.0827E+03
1603, 7.2091E+01, 0.0000E+00, 1.1024E+03
1633, 7.2091E+01, 0.0000E+00, 1.1220E+03
1661, 7.2091E+01, 0.0000E+00, 1.1417E+03
1689, 7.2091E+01, 0.0000E+00, 1.1614E+03
1717, 7.2091E+01, 0.0000E+00, 1.1811E+03
1745, 7.2091E+01, 0.0000E+00, 1.2008E+03
1773, 7.2091E+01, 0.0000E+00, 1.2205E+03
1801, 7.2091E+01, 0.0000E+00, 1.2402E+03
1829, 7.2091E+01, 0.0000E+00, 1.2598E+03
1857, 7.2091E+01, 0.0000E+00, 1.2795E+03
1885, 7.2091E+01, 0.0000E+00, 1.2992E+03
1913, 7.2091E+01, 0.0000E+00, 1.3189E+03
1941, 7.2091E+01, 0.0000E+00, 1.3386E+03
1971, 7.2091E+01, 0.0000E+00, 1.3583E+03
1999, 7.2091E+01, 0.0000E+00, 1.3780E+03
2027, 7.2091E+01, 0.0000E+00, 1.3976E+03
2055, 7.2091E+01, 0.0000E+00, 1.4173E+03
2083, 7.2091E+01, 0.0000E+00, 1.4370E+03
2111, 7.2091E+01, 0.0000E+00, 1.4567E+03
2139, 7.2091E+01, 0.0000E+00, 1.4764E+03
2167, 7.2091E+01, 0.0000E+00, 1.4961E+03
2195, 7.2091E+01, 0.0000E+00, 1.5157E+03
2223, 7.2091E+01, 0.0000E+00, 1.5354E+03
2251, 7.2091E+01, 0.0000E+00, 1.5551E+03
2279, 7.2091E+01, 0.0000E+00, 1.5748E+03
2309, 7.2091E+01, 0.0000E+00, 1.5945E+03
2337, 7.2091E+01, 0.0000E+00, 1.6142E+03
2365, 7.2091E+01, 0.0000E+00, 1.6339E+03
2393, 7.2091E+01, 0.0000E+00, 1.6535E+03
2421, 7.2091E+01, 0.0000E+00, 1.6732E+03
2449, 7.2091E+01, 0.0000E+00, 1.6929E+03
2477, 7.2091E+01, 0.0000E+00, 1.7126E+03
2505, 7.2091E+01, 0.0000E+00, 1.7323E+03
2533, 7.2091E+01, 0.0000E+00, 1.7520E+03
2561, 7.2091E+01, 0.0000E+00, 1.7717E+03
2589, 7.2091E+01, 0.0000E+00, 1.7913E+03
```

```
        2617, 7.2091E+01, 0.0000E+00, 1.8110E+03
        2647, 7.2091E+01, 0.0000E+00, 1.8307E+03
        2675, 7.2091E+01, 0.0000E+00, 1.8504E+03
        2703, 7.2091E+01, 0.0000E+00, 1.8701E+03
        2731, 7.2091E+01, 0.0000E+00, 1.8898E+03
        2759, 7.2091E+01, 0.0000E+00, 1.9094E+03
        2787, 7.2091E+01, 0.0000E+00, 1.9291E+03
        2815, 7.2091E+01, 0.0000E+00, 1.9488E+03
        2843, 7.2091E+01, 0.0000E+00, 1.9685E+03
        2871, 7.2091E+01, 0.0000E+00, 1.9882E+03
        2899, 7.2091E+01, 0.0000E+00, 2.0079E+03
        2927, 7.2091E+01, 0.0000E+00, 2.0276E+03
        2955, 7.2091E+01, 0.0000E+00, 2.0472E+03
        2985, 7.2091E+01, 0.0000E+00, 2.0669E+03
        3013, 7.2091E+01, 0.0000E+00, 2.0866E+03
        3041, 7.2091E+01, 0.0000E+00, 2.1063E+03
        3073, 7.2091E+01, 0.0000E+00, 2.1260E+03
**
**********************************************************
** Elements in the right guideway
*
**********************************************************
*ELEMENT, TYPE=B31, ELSET=ERIGHT
1,10,38
2,38,66
3,66,94
4,94,124
5,124,152
6,152,180
7,180,208
8,208,236
9,236,264
10,264,292
11,292,320
12,320,348
13,348,376
14,376,404
15,404,432
16,432,462
17,462,490
18,490,518
19,518,546
20,546,574
21,574,602
22,602,630
23,630,658
24,658,686
25,686,714
26,714,742
27,742,770
28,770,800
29,800,828
30,828,856
```

```
31,856,884
32,884,912
33,912,940
34,940,968
35,968,996
36,996,1024
37,1024,1052
38,1052,1080
39,1080,1108
40,1108,1138
41,1138,1166
42,1166,1194
43,1194,1222
44,1222,1250
45,1250,1278
46,1278,1306
47,1306,1334
48,1334,1362
49,1362,1390
50,1390 ,1418
51,1418,1446
52,1446,1476
53,1476,1504
54,1504,1534
55,1534,1566
56,1566,1594
57,1594,1622
58,1622,1652
59,1652,1680
60,1680,1708
61,1708,1736
62,1736,1764
63,1764,1792
64,1792,1820
65,1820,1848
66,1848,1876
67,1876,1904
68,1904,1932
69,1932,1960
70,1960,1990
71,1990,2018
72,2018,2046
73,2046,2074
74,2074,2102
75,2102,2130
76,2130,2158
77,2158,2186
78,2186,2214
79,2214,2242
80,2242,2270
81,2270,2298
82,2298,2328
83,2328,2356
```

```
84,2356,2384
85,2384,2412
86,2412,2440
87,2440,2468
88,2468,2496
89,2496,2524
90,2524,2552
91,2552,2580
92,2580,2608
93,2608,2636
94,2636,2666
95,2666,2694
96,2694,2722
97,2722,2750
98,2750,2778
99,2778,2806
100,2806,2834
101,2834,2862
102,2862,2890
103,2890,2918
104,2918,2946
105,2946,2974
106,2974,3004
107,3004,3032
108,3032,3062
**
**Elements of the left side
**
*ELEMENT, TYPE=B31, ELSET=ELEFT
109,19,47
110,47,75
111,75,105
112,105,133
113,133,161
114,161,189
115,189,217
116,217,245
117,245,273
118,273,301
119,301,329
120,329,357
121,357,385
122,385,413
123,413,443
124,443,471
125,471,499
126,499,527
127,527,555
128,555,583
129,583,611
130,611,639
131,639,667
132,667,695
```

```
133,695,723
134,723,751
135,751,781
136,781,809
137,809,837
138,837,865
139,865,893
140,893,921
141,921,949
142,949,977
143,977,1005
144,1005,1033
145,1033,1061
146,1061,1089
147,1089,1119
148,1119,1147
149,1147,1175
150,1175,1203
151,1203,1231
152,1231,1259
153,1259,1287
154,1287,1315
155,1315,1343
156,1343,1371
157,1371,1399
158,1399,1427
159,1427,1457
160,1457,1485
161,1485,1513
162,1513,1545
163,1545,1575
164,1575,1603
165,1603,1633
166,1633,1661
167,1661,1689
168,1689,1717
169,1717,1745
170,1745,1773
171,1773,1801
172,1801,1829
173,1829,1857
174,1857,1885
175,1885,1913
176,1913,1941
177,1941,1971
178,1971,1999
179,1999,2027
180,2027,2055
181,2055,2083
182,2083,2111
183,2111,2139
184,2139,2167
185,2167,2195
```

```
186,2195,2223
187,2223,2251
188,2251,2279
189,2279,2309
190,2309,2337
191,2337,2365
192,2365,2393
193,2393,2421
194,2421,2449
195,2449,2477
196,2477,2505
197,2505,2533
198,2533,2561
199,2561,2589
200,2589,2617
201,2617,2647
202,2647,2675
203,2675,2703
204,2703,2731
205,2731,2759
206,2759,2787
207,2787,2815
208,2815,2843
209,2843,2871
210,2871,2899
211,2899,2927
212,2927,2955
213,2955,2985
214,2985,3013
215,3013,3041
216,3041,3073
**
**Definition of the elements used for the diaphragms
**
*ELEMENT,TYPE=B31,ELSET=DIAPH
300,94,105
301,432,443
302,770,781
303,1108,1119
304,1446,1457
305,1622,1633
306,1960,1971
307,2298,2309
308,2636,2647
309,2974,2985
**
** Definition of the Cross Section of the guideway
beams
**
*BEAM
SECTION,SECTION=RECT,ELSET=ERIGHT,MATERIAL=M0001001
 52,73
 1.000E+00, 0.000E+00,  0.000E+00
```

```
*BEAM
SECTION,SECTION=RECT,ELSET=ELEFT,MATERIAL=M0001001
 52,73
 1.000E+00,  0.000E+00,  0.000E+00
**
** Definition of the Cross Section of the diaphragms
**
*BEAM
SECTION,SECTION=RECT,ELSET=DIAPH,MATERIAL=M0001002
14,21
 0.000E+00,  0.000E+00,  -1.000E+00
**
** Definition of the concrete material
**
*MATERIAL,NAME=M0001001
*ELASTIC,TYPE=ISOTROPIC
 5.000E+06, 1.500E-01
*DENSITY
1.25000E-4
*TRANSVERSE SHEAR STIFFNESS
 2.17E+06
*MATERIAL,NAME=M0001002
*ELASTIC,TYPE=ISOTROPIC
 5.000E+06, 1.500E-01
*DENSITY
1.25000E-4
*TRANSVERSE SHEAR STIFFNESS
 2.17E+06
**
************************************************
** Prestressed rebar inside the guidewaay beams *
************************************************
**
**Generation of the element set for the positive
prestress rebars
**
*ELSET,ELSET=ALL
ERIGHT,ELEFT
**
**Generation of the element set for the negative
prestress rebars
**
*ELSET,ELSET=NRRIGHT,GENERATE
45,64,1
*ELSET,ELSET=NRLEFT,GENERATE
152,172,1
*ELSET,ELSET=NEGREINF
NRRIGHT,NRLEFT
**
** Positive Reinforcement
**
*REBAR,ELEMENT=BEAM,MATERIAL=HSST,GEOMETRY=ISOPARAMETR
IC,NAME=BOTTOM
```

```
ALL,0.514,-20.5,-37.5
ALL,0.514,-13.0,-37.5
ALL,0.514,-7.00,-37.5
ALL,0.514,0.00,-37.5
ALL,0.514,7.0,-37.5
ALL,0.514,13.0,-37.5
ALL,0.514,20.5,-37.5
*MATERIAL,NAME=HSST
*ELASTIC
 27.E6
**
**Intial condition for the positive prestressed bars
**
*INITIAL CONDITIONS,TYPE=STRESS,REBAR
ALL,BOTTOM,144000.
**
** Negative Reinforcement Bars
**
*REBAR,ELEMENT=BEAM,MATERIAL=GFRP,GEOMETRY=ISOPARAMETR
IC,NAME=NEGTEN
NEGREINF,.9,-20.5,37.5
NEGREINF,.9,-13.0,37.5
NEGREINF,.9,-7.00,37.5
NEGREINF,.9,0.00,37.5
NEGREINF,.9,7.0,37.5
NEGREINF,.9,13.0,37.5
NEGREINF,.9,20.5,37.5
*MATERIAL,NAME=GFRP
*ELASTIC
60.E6
**
**Intial condition for the negative prestressed bars
**
*INITIAL CONDITIONS,TYPE=STRESS,REBAR
NEGREINF,NEGTEN,103000.
**
*** Following modifications are done by Mao since Nov.
1, 1993
**
**
*NSET, NSET=NTRACK_R
 1534, 1622
*NSET, NSET=NTRACK_R, GENERATE
 3062, 3062, 28
 3004, 3032, 28
 2666, 2974, 28
 2328, 2636, 28
 1990, 2298, 28
 1652, 1960, 28
 1566, 1594, 28
 1476, 1504, 28
 1138, 1446, 28
  800, 1108, 28
```

```
  462,  770, 28
  124,  432, 28
   10,   94, 28
*NMAP, TYPE=RECTANGULAR, NSET=NTRACK_R
  0.0, 0.0, 0.0

 1E-12, 1E-12, 1.0
*NMAP, TYPE=RECTANGULAR, NSET=NTRACK_R
 -72.1, 0.0, 0.0

  1.0, 1.0, 1.0
*NSET, NSET=NTRACK_L, GENERATE
  19,   75, 28
 105,  413, 28
 443,  751, 28
 781, 1089, 28
1119, 1427, 28
1457, 1513, 28
1545, 1545, 28
1575, 1603, 28
1633, 1941, 28
1971, 2279, 28
2309, 2617, 28
2647, 2955, 28
2985, 3041, 28
3073, 3073, 28
*NMAP, TYPE=RECTANGULAR, NSET=NTRACK_L
  0.0, 0.0, 0.0

 1E-12, 1E-12, 1.0
*NMAP, TYPE=RECTANGULAR, NSET=NTRACK_L
  72.1, 0.0, 0.0

  1.0, 1.0, 1.0
**
** Equilibriate the applied prestressed force
**
*NSET, NSET=VEHICLE, GENERATE
 20001, 29999, 1
*STEP,NLGEOM
*STATIC
 0.5, 1.0, 0.5
*RESTART,WRITE, F=100
*MONITOR, NODE=20100, DOF=3
*PRESTRESS HOLD
ALL,BOTTOM,NEGREINF,NEGTEN
**
**Boundary Conditions
**
*NSET,NSET=HINGE
1534,1545
*NSET,NSET=ROLLER
10,19,3062,3073
```

```
*BOUNDARY
HINGE,1,3
*BOUNDARY
ROLLER,1,2
*BOUNDARY
 CAR_CENT, 5,6
 N_BOGIE,  6,6
 ENDNODES, 1,6
  VEHICLE, 1,1
*BOUNDARY, TYPE=VELOCITY
  VEHICLE, 3,3, 0.0
*DLOAD
 V_MASS, GRAV, 386., 0.0, -1., 0.0
 E_CAR , GRAV, 386., 0.0, -1., 0.0
*NODE PRINT, NSET=NTRACK, F=4, TOTALS=YES
 RF,
*NSET, NSET=CENTER
 20100, 20200
**NODE PRINT, NSET=CENTER, F=1
** U1, V1, A1
*NSET, NSET=GWNODES
RIGHT,LEFT
*NODE FILE, NSET=GWNODES,F=1
U
*ELSET, ELSET=PRINT
 20012, 20014, 20022, 20024
*ELSET, ELSET=PRINT
 MAG_L, MAG_R,
*END STEP
**
**Original dynamic loading for the guideway
**
*STEP, NLGEOM, INC=250
*DYNAMIC, DIRECT, NOHAF
 0.003, 0.74
*RESTART, WRITE,F=7
*PRINT, CONTACT=YES
*BOUNDARY, TYPE=VELOCITY
 VEHICLE, 3,3, 5600.0
*NODE FILE, F=7
 U
*END STEP
```

REPORT DOCUMENTATION PAGE

Form Approved
OMB No. 0704-0188

1. AGENCY USE ONLY *(Leave blank)*	2. REPORT DATE	3. REPORT TYPE AND DATES COVERED
	December 1995	Final report

4. TITLE AND SUBTITLE
A Finite Element Model for Assessment of Maglev Vehicle/Guideway Interaction

5. FUNDING NUMBERS

6. AUTHOR(S)
James C. Ray, Yazmin Seda-Sanabria, Mostafiz R. Chowdhury, Stanley C. Woodson

7. PERFORMING ORGANIZATION NAME(S) AND ADDRESS(ES)
U.S. Army Engineer Waterways Experiment Station
3909 Halls Ferry Road, Vicksburg, MS 39180-6199

8. PERFORMING ORGANIZATION REPORT NUMBER
Technical Report SL-95-23

9. SPONSORING/MONITORING AGENCY NAME(S) AND ADDRESS(ES)
U.S. Army Engineer Division, Huntsville
P.O. Box 1600
Huntsville, AL 35807-4301

10. SPONSORING/MONITORING AGENCY REPORT NUMBER

11. SUPPLEMENTARY NOTES
Available from National Technical Information Service, 5285 Port Royal Road, Springfield, VA 22161.

12a. DISTRIBUTION/AVAILABILITY STATEMENT
Approved for public release; distribution is unlimited.

12b. DISTRIBUTION CODE

13. ABSTRACT *(Maximum 200 words)*

A finite element methodology is presented for the assessment of the dynamic interaction between a rapidly moving magnetically levitated vehicle and its supporting guideway structure, known as vehicle/guideway interaction (VGI). The methodology is validated through comparison to two other analytical methodologies. Its application and usefulness for VGI studies are demonstrated through application to an actual maglev system design.

14. SUBJECT TERMS
High-speed ground transportation
Magnetic levitation
Maglev
Vehicle/guideway interaction

15. NUMBER OF PAGES
78

16. PRICE CODE

17. SECURITY CLASSIFICATION OF REPORT	18. SECURITY CLASSIFICATION OF THIS PAGE	19. SECURITY CLASSIFICATION OF ABSTRACT	20. LIMITATION OF ABSTRACT
UNCLASSIFIED	UNCLASSIFIED		